# TRANSFER FUNCTIONS WITH POSITIVE IMPULSE RESPONSE: FEEDBACK CONTROLLER DESIGN AND APPLICATION TO COOPERATIVE ADAPTIVE CRUISE CONTROL

A THESIS SUBMITTED TO
THE GRADUATE SCHOOL OF NATURAL AND APPLIED SCIENCES
OF
MIDDLE EAST TECHNICAL UNIVERSITY

BY

İBRAHIM TAYYIP İŞLER

IN PARTIAL FULFILLMENT OF THE REQUIREMENTS
FOR
THE DEGREE OF MASTER OF SCIENCE
IN
ELECTRICAL AND ELECTRONICS ENGINEERING

SEPTEMBER 2021

Approval of the thesis:

**TRANSFER FUNCTIONS WITH POSITIVE IMPULSE RESPONSE: FEEDBACK CONTROLLER DESIGN AND APPLICATION TO COOPERATIVE ADAPTIVE CRUISE CONTROL**

submitted by **İBRAHIM TAYYIP İŞLER** in partial fulfillment of the requirements for the degree of **Master of Science in Electrical and Electronics Engineering Department, Middle East Technical University** by,

Prof. Dr. Halil Kalıpçılar
Dean, Graduate School of **Natural and Applied Sciences** _____

Prof. Dr. İlkay Ulusoy
Head of Department, **Electrical and Electronics Engineering** _____

Prof. Dr. Klaus Werner Schmidt
Supervisor, **Electrical and Electronics Engineering, METU** _____

**Examining Committee Members:**

Assoc. Prof. Dr. Emre Özkan
Electrical and Electronics Engineering, METU _____

Prof. Dr. Klaus Werner Schmidt
Electrical and Electronics Engineering, METU _____

Assist. Prof. Dr. Mustafa Mert Ankaralı
Electrical and Electronics Engineering, METU _____

Assoc. Prof. Dr. Çağlar Başlamışlı
Mechanical Engineering, Hacettepe University _____

Assist. Prof. Dr. Halit Ergezer
Mechatronics Engineering, Çankaya University _____

Date: 07.09.2021

**I hereby declare that all information in this document has been obtained and presented in accordance with academic rules and ethical conduct. I also declare that, as required by these rules and conduct, I have fully cited and referenced all material and results that are not original to this work.**

Name, Surname: İbrahim Tayyip İşler

Signature :

# ABSTRACT

## TRANSFER FUNCTIONS WITH POSITIVE IMPULSE RESPONSE: FEEDBACK CONTROLLER DESIGN AND APPLICATION TO COOPERATIVE ADAPTIVE CRUISE CONTROL

İşler, İbrahim Tayyip
M.S., Department of Electrical and Electronics Engineering
Supervisor: Prof. Dr. Klaus Werner Schmidt

September 2021, 73 pages

Driver assistance systems are increasingly employed to replace human driver functionality. Cooperative adaptive cruise control (CACC) automates the longitudinal vehicle motion to support safe vehicle following using distance measurements and state information communicated among vehicles. A basic requirement when using CACC is to attenuate fluctuations along vehicle strings, which is captured by the formal condition of string stability. Hereby, different notions of string stability exist in the literature based on different operator norms.

In this thesis, a string stability condition based on the L-infinity norm, denoted as strict $L_\infty$ string stability is used. This condition can be fulfilled by designing a CACC feedback loop, where the input/output behavior of the CACC system has positive impulse response. Accordingly, the main contribution of this thesis is the development of sufficient conditions for achieving a positive impulse response. These conditions are then used to formulate an optimization problem, whose solution provides suitable controller parameters for ensuring strict $L_\infty$ string stability. The practicability

of the proposed method is validated by simulation experiments with realistic vehicle parameters. In addition, it is shown that the proposed method is robust to additional communication delay and actuator delay, which are generally encountered in real-life CACC systems.

Keywords: Cooperative Adaptive Cruise Control, String Stability, Heterogeneous Vehicle Strings, Positive Impulse Response

# ÖZ

## POZİTİF DÜRTÜ TEPKİLİ TRANSFER FONKSİYONLARI: GERİBESLEMELİ KONTROLCÜ TASARIMI VE KOOPERATİF ADAPTİF SEYİR KONTROLÜ UYGULAMASI

İşler, İbrahim Tayyip
Yüksek Lisans, Elektrik ve Elektronik Mühendisliği Bölümü
Tez Yöneticisi: Prof. Dr. Klaus Werner Schmidt

Eylül 2021 , 73 sayfa

Sürücü yardım sistemleri, insan sürücü işlevselliğinin yerini almak için giderek daha fazla kullanılmaktadır. Kooperatif adaptif seyir kontrolü (CACC), araçlar arasında iletilen mesafe ölçümlerini ve durum bilgilerini kullanarak güvenli araç takibini desteklemek için boylamasına araç hareketini otomatikleştirir. CACC kullanırken temel bir gereklilik, zincir stabilitesinin formel koşulu tarafından yakalanan araç zincirleri boyunca dalgalanmaları azaltmaktır. Bu vesileyle, literatürde farklı operatör normlarına dayanan farklı zincir stabilite kavramları mevcuttur.

Bu tezde, L-sonsuz normuna dayalı mutlak $L_\infty$ zincir stabilite diye tabir edilen bir zincir stabilite koşulu kullanılmıştır. Bu koşul, giriş/çıkış davranışının pozitif dürtü yanıtına sahip olduğu bir CACC geri besleme döngüsü tasarlanarak yerine getirilebilir. Bunun üzerine ilerlenerek bu tezin ana katkısı pozitif dürtü yanıtının elde edilmesi için yeterli koşulların geliştirilmesi olmuştur. Bu koşullar daha sonra çözümü mutlak $L_\infty$ zincir stabilitesini garanti eden uygun kontrolcü parametrelerini sağlayan bir optimizasyon probleminin formülize edilmesinde kullanılmıştır. Öne sürülen yöntemin

uygulanabilirliği gerçekçi araç parametreleri ile gerçekleştirilen benzetim deneyleriyle doğrulanmıştır. Ayrıca, öne sürülen yöntemin, gerçek hayatta CACC sistemlerinde genellikle karşılaşılan ekstra iletişim ve eyleyici gecikmelerine karşı gürbüz yapıda olduğu gösterilmiştir.

Anahtar Kelimeler: Kooperatif Adaptif Seyir Kontrolü, Zincir-Stabilite, Heterojen Araç Zincirleri, Pozitif Dürtü Tepkisi

*to the Truth...*

## ACKNOWLEDGMENTS

I would like to express my deepest gratitude to my supervisor Prof. Dr. Klaus Werner Schmidt for his constant support, unique guidance and uplifting encouragement throughout my graduate study under his supervision.

For their perceptive comments, and criticism, I would also like to thank the committee members.

I am grateful to my company and colleagues for their encouragement and understanding during my graduate studies.

I would like to thank my friends Muhammed Yusuf Candan and Mustafa Murat Sezer for their sincere and caring advice throughout my academic journey.

I would like to express my foremost thanks to my ever loving mother Sema, generous and reliable father Ahmet Sami, lovely sister and genuinely protective brother Amine Berra and Talha, and to my compassionate grandparents, for everything they made to bring me up to this day.

I owe my loving thanks to my beloved wife Reyyan because without her love, support, and patience, I would not have been able to cope with work and graduate studies simultaneously. I shall always remember her trust in me.

All praise and gratitude is due to Allah, by whose favor good deeds are accomplished.

## TABLE OF CONTENTS

# LIST OF TABLES

TABLES

## LIST OF FIGURES

FIGURES

## LIST OF ABBREVIATIONS

| | |
|---|---|
| CC | Cruise Control |
| ACC | Adaptive Cruise Control |
| CACC | Coopertative Adaptive Cruise Control |
| SS | String Stability |
| MPC | Model Predictive Control |
| IR | Impulse Response |
| PIR | Positive Impulse Response |
| LPF | Low-Pass Filter |
| PI | Proportional-Integral |
| PD | Proportional-Derivative |
| PID | Proportional-Integral-Derivative |
| AF | Acceleration Feedforward |
| PAF | Predicted Acceleration Feedforward |
| ISF | Input Signal Feedforward |
| BIBO | Bounded Input Bounded Output |

## LIST OF VARIABLES

| | |
|---|---|
| $x$ | Position |
| $v$ | Velocity |
| $a$ | Acceleration |
| $L$ | Vehicle length |
| $d$ | Intervehicle distance |
| $r$ | Intervehicle distance at standstill |
| $h$ | Headway time |
| $\phi$ | Actuator time delay |
| $\tau$ | Driveline dynamics |
| $\theta$ | Communication delay |
| $G$ | Longitudinal vehicle dynamics transfer function |
| $C$ | Feedback controller transfer function |
| $K_p$ | Proportional gain |
| $K_d$ | Derivative gain |
| $F$ | Feedforward filter transfer function |
| $H$ | Constant time-gap transfer function |
| $D$ | Communication delay transfer function |
| $\Gamma$ | Closed loop transfer function between vehicles |

# CHAPTER 1

# INTRODUCTION

One of the trending topics of the last decade has been autonomous vehicles. Major automotive companies are already in a rivalry in achieving higher levels of autonomy. In fact, there are already significant examples of autonomous driving trials such as Google's Waymo and others. Still, there is quite some work to be undertaken for completely autonomous driving functionality. In addition, the difficulties and limitations faced whilst trying to solve control issues in autonomous driving systems not only relate to necessity of further studies in control theory to develop techniques addressing subject specific matters, but also to other interdisciplinary study areas, such as 5G communication.

Dividing the problem of autonomous driving into subproblems, one of the major issues is the control of longitudinal motion. Longitudinal control, i.e. applying the throttle or brake action, constitutes a huge portion of the entire motion taking place in traffic. Thus, it needs to be studied painstakingly. Every step to be taken in this field of study will determine how much more we can lessen the footprints to be left to the future. By now, it has become evident to the researchers [1], [2] that closing the inter-vehicle distance in vehicle platoons has promising results, such as increase in traffic throughput, decrease in energy consumption, and savings of time. Yet, how this goal can safely be achieved still remains as an open area of research. Specifically, cooperative adaptive cruise control (CACC) offers a highly efficient and secure solution to the question of controlling longitudinal vehicle dynamics. In short CACC, uses both sensor measurements such as distance and velocity and communicated state information between vehicles in order to enable driving at small inter-vehicle distances, hence yielding efficiency in traffic flow and fuel consumption.

There have been many studies on this subject aiming both theoretical development and practical implementation. In some studies, the means of communication which are the underlying basis of CACC and its requirements have been discussed. The matter of communicating the feedforward signals of predecessor vehicles will not be in the scope of our study. Rather, we will be solely concentrating on how to synthesize robust controllers that can handle various situations at real-life scenario. For a quick review on the topic of how vehicle to vehicle (V2V) communication is sustained Dey *et al.* [3] can be referred. Also Darbha *et al.*'s [4] is enlightening for gaining some insight into the benefits of V2V communication in CACC. The study carried out by Xing *et al.* [5] makes it clear how communication delays can be critical and its compensation can yield significant improvements. For a more holistic view of the subject Wang *et al.*'s survey [6] can be consulted.

Regarding the practical implementation of CACC, Ploeg *et al.* [7] clearly showed the possibility of increasing traffic throughput via lower distances between vehicles by proving theoretical work to be true in the field with a test fleet of vehicles. Furthermore, Bayezit *et al.* [8] also managed to implement CACC in the Grand Cooperative Driving Challange (GCDC). In the United States, there have been several attempts by the United States Department of Transportation who took a comprehensive initiative to establish and see the full potential of connected vehicle concept. A recent study [9] brought engineers from different major car manufacturer companies together to test and see the outcomes of utilization of CACC to its full capacity. Yet, there is still a lot of work to be done both in theory and practice.

CACC can be established through a variety of control schemes and as long as they serve the purpose and guarantee safe driving, they are all considered to be conforming. As a constituent component, each control policy comes with a spacing policy that determines the desired distance between vehicles in a string. On the one hand, there is work on the constant gap policy, where vehicles travel at a constant distance independent of the vehicle velocity [10, 11]. On the other hand, a large body of the existing work on CACC focuses on a variable spacing policy, where the desired distance increases linearly with the vehicle velocity depending on a headway time constant [12–14]. In this thesis, we focus on the variable spacing policy due to its higher relevance in practice.

All control methods utilized for CACC aim to grant a more comfortable and efficient longitudinal driver unit while at the same time trying not to compromise any budget from robustness or safety. In this context, string stability is an important condition to fulfill the described goal. Intuitively, string stability ensures that fluctuations in a vehicle string are attenuated along the string. Wang *et al.* [15] reviewed some of the related approaches. For instance, Zhu *et al.* in [16], focused on uncertainties and heterogeneity of vehicle strings, hence, put forth adaptive optimal control techniques as a solution to CACC problem. Zhou *et al.* [17], developed a specific model predictive control (MPC) approach to achieve string stability goal.

When considering string stability, it has to be noted that different definitions of string stability exist. Specifically, [1] introduces the general notion of strict $L_p$ string stability and puts forward that the special cases of strict $L_2$ and strict $L_\infty$ string stability are of practical use. $L_2$ string stability ensures the attenuation of the $L_2$ norm (energy content) , whereas strict $L_\infty$ string stability guarantees the attenuation of the $L_\infty$ norm (maximum amplitude) of a chosen output signal along a vehicle string. Zhu *et al.* in [16], considered the $L_2$ string stability definition and tried to find the minimum headway times by sum of squares programming. Zhou *et al.* [17], considered both $L_2$ and $L_\infty$ string stability definitions with MPC. In the literature, frequency domain analysis and tools to suffice $L_2$ string stability are discussed thoroughly. However, there is an obvious shortage of studies in the field of time domain analysis for fulfilling strict $L_\infty$ string stability condition. Yet, it possesses potentially a more powerful type of string stability.

The main contribution of this thesis work comes right at this point, providing a unique method for fulfilling strict $L_\infty$ string stability with an additional robustness feature of yielding positive impulse responses. The method also gives the user an opportunity to turn the headway time constant into one of the optimization parameters. In order to validate the method we propose, there have been several types of tests carried out. We first experiment with different driveline dynamics constants to show that our method can manage a spectrum of strings and vehicles. Then, we move on to tests regarding the delays to analyze the method's robustsness and viability. Ultimately, the method proposed was observed to be capable of dealing with significant amount of cases and realistic values even under non-zero delay values.

After the introduction chapter, there will be three main chapters to this thesis in which the necessary concepts, the problem, and the results attained will be shared in an orderly fashion. In the second chapter, background is divided into three subjects. Two of the background subjects constitute directly the fundamental elements of a CACC. The third section in the background chapter lays out the unprecedented solution approach which we are trying to adapt for the CACC problem. In the third chapter, what can also be labeled as the body of the thesis work regarding CACC is brought under attention. The fourth presents the results and comments on them. Finally, the thesis concludes with remarks and thoughts on prospective studies which can be built upon this work or may benefit from the results observed.

# CHAPTER 2

# BACKGROUND

## 2.1 Cooperative Adaptive Cruise Control

Cooperative adaptive cruise control (CACC) is an extension of the commercially available adaptive cruise control (ACC) systems with a feedforward signal added to the control loop, increasing robustness and yielding a new notion of stability named string stability.

Block diagrams for both ACC and CACC, and, highlighted in blue, the evolution of ACC to CACC with feedforward path addition are shown in Figure 2.1. Briefly, $G_i$ represents the longitudinal vehicle dynamics, $C_i$ is the feedback controller generating the acceleration and deceleration actions in the loop and, $F_i$ is the feedforward transfer function which enables the follower vehicles to replicate the actions of their predecessors much quicker than they do in the case of ACC.

The general setting of CACC is illustrated in Figure 2.2. In CACC, vehicles form a string to achieve a seamless and harmonious longitudinal motion while observing a certain type of inter-vehicle spacing policy. In the literature, generally, a policy named '*constant time gap*' is practiced which simply means maintaining a distance proportional to the velocity of the string. This proportionality constant is also referred as '*headway time*'. In Figure 2.3, the constant time gap spacing policy is illustrated.

Assuming a constant gap between all vehicles along the string at standstill (2.3), the aim of CACC is to maximize the number of vehicles travelling in unit time (traffic throughput) and to minimize fuel consumption by minimizing the inter-vehicle distance. In short, in the ideal case, the whole string of vehicles would have acted as one

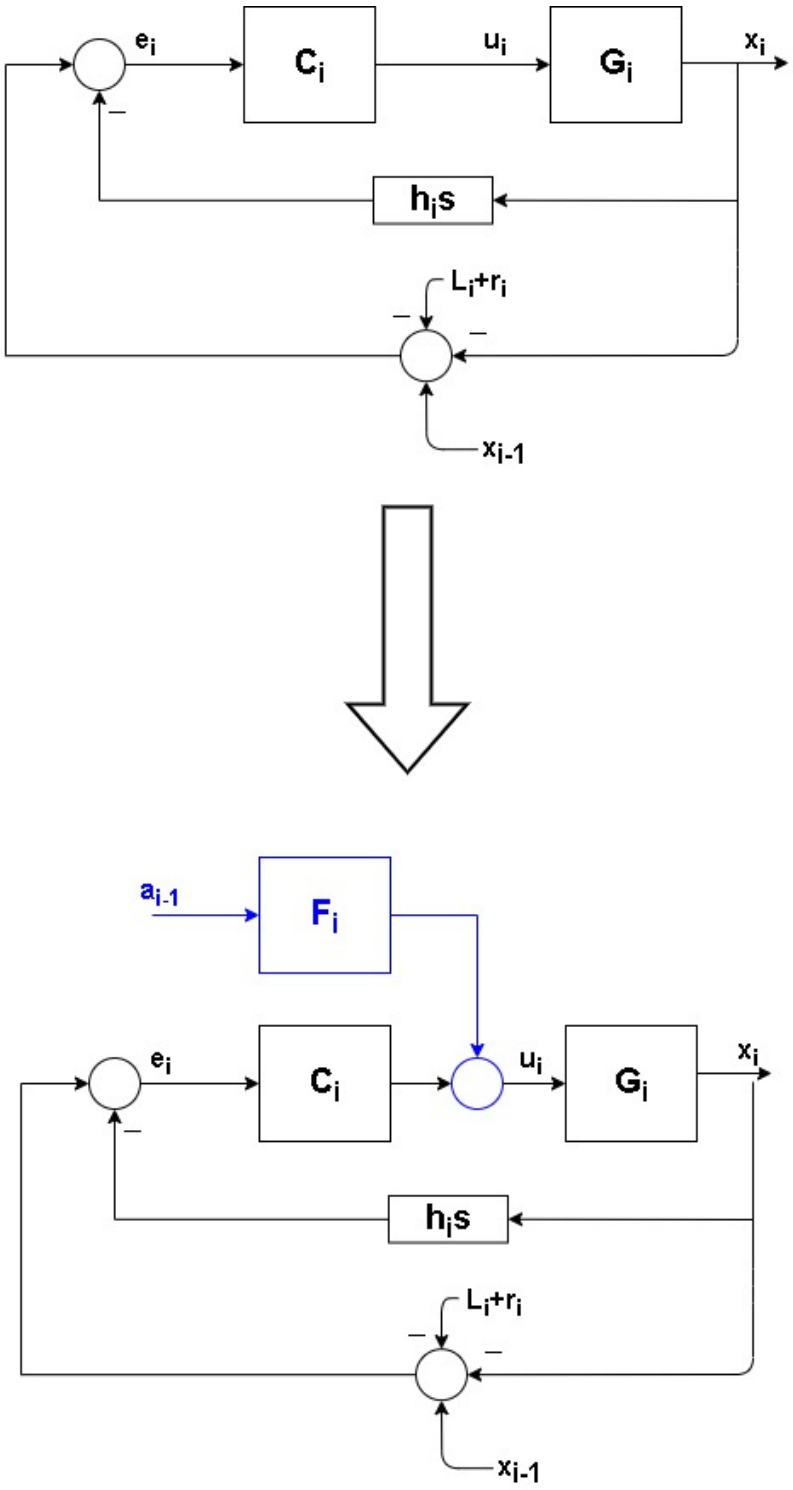


Figure 2.1: ACC and CACC

body by all vehicles applying the changes of the velocity of their predecessor vehicles instantaneously with zero time gap yielding zero velocity tracking error. Thence,

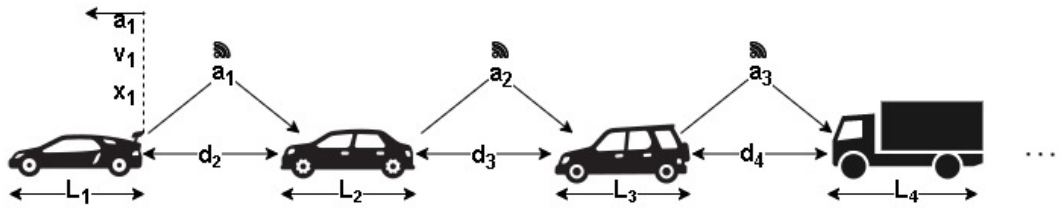


Figure 2.2: CACC Vehicle String Structure

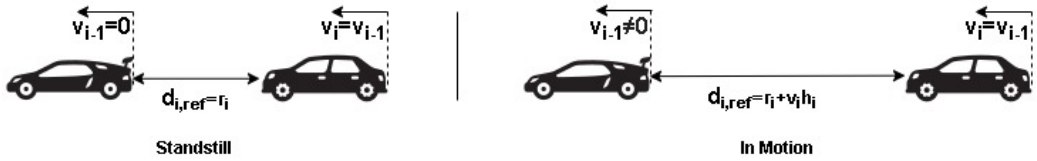


Figure 2.3: Constant Time Gap Policy

the inter-vehicle distance would have been minimized to the initial standstill constant distance. However, there are limiting factors in reality, such as communication and actuator delays and, bounds on the control inputs. Therefore, the inter-vehicle distance and how quick vehicles track their predecessors' velocities will have to be traded off for robustness and safety.

In a predecessor-follower type CACC application, the plant is the whole chain of vehicles. In practice, every individual vehicle other than the leader is responsible for implementing the changes in longitudinal motion that it receives from its predecessor as a reference signal in a specific fashion, which can be characterized with a certain type of transient behavior too. So, a string stable CACC will be achieved if and only if all follower vehicles are controlled meeting the transient response requirements. Right then and there, we suggest and assume that designing controllers yielding positive impulse responses will be a feasible and highly effective way of establishing CACC.

In the definition of CACC problem, only the longitudinal motion is defined and dealt with. For practical purposes, number of vehicles in a string is left unlimited. Also the type of strings can be divided into two categories as homogeneous and heterogeneous strings. In homogeneous strings all members of the string are assumed to be

identical vehicles. This definition makes certain analysis easier and brings simplicity to the problem formulation, in that, the vehicle dynamics difference is no longer existent. On the other hand, in heterogeneous strings, every vehicle has to consider its predecessor's driveline dynamics while controlling its own attitude of acceleration or deceleration. So the dynamic difference has to be accounted for in controller design.

The vehicle string can be depicted as in Figure 2.2. Therein, $L_i$ denotes the length of $i^{th}$ vehicle. The distance between vehicles at any time instant is $d_i$. Lastly, taking the rear bumpers as the reference point we denote the position, velocity and acceleration of $i^{th}$ vehicle by $x_i, v_i$ and $a_i$ respectively.

To begin with, the intervehicle spacing policy has to be determined before designing a CACC. To this end, constant time gap is the most frequently encountered approach in literature. It is a simple and intuitive way to set a distancing rule that fits very well to the problem nature. There have been other spacing policies suggested in the literature too. However, we will also stick with the constant time gap spacing policy (Figure 2.3) and implement it in our problem definition.

Letting $r_i$ denote the distance between vehicles at standstill (i.e. when $v_i = 0, i = 1, 2, ..., n$), the constant time gap spacing policy is given as

$$d_{i,ref} = r_i + h_i v_i. \tag{2.1}$$

In steady state, the distance between vehicles will settle at $d_{i,ref}$. On the other hand, in the transient part, where the predecessor vehicle adopts to a new velocity, the actual distance between subsequent vehicles will be defined as

$$d_i = x_{i-1} - x_i - L_i. \tag{2.2}$$

The difference between the actual distance signal and the reference distance value will define the spacing error.

$$e_i = d_i - d_{i,ref} = x_{i-1} - x_i - L_i - r_i - h_i v_i \tag{2.3}$$

This positional error will be controlled by the CACC in a way that guarantees collision-free longitudinal driving under any practical acceleration or deceleration behavior.

It must also be noted that the constant time gap policy can be expressed in s-domain

as

$$H_i(s) = 1 + h_i s. \tag{2.4}$$

This form of constant time gap policy will be used in s-domain analysis of the closed loop transfer function and it will be seen that the headway times of each vehicle introduce a unique pole of its own in the vehicle-to-vehicle transfer function.

Longitudinal dynamics of a vehicle is much more simpler than its lateral dynamics. Taking the throttle and brake actions, i.e. acceleration, as input to the system, the output is defined as the longitudinal position of the vehicle. The transfer function in Equation (2.5) is validated for a wide range of driving scenarios [18] and its usefulness is acknowledged in the recent academic works [13, 19, 20]. It is, in fact, a simplified model obtained from a more complex one by applying feedback linearization [7, 21, 22].

$$G_i(s) = \frac{Y_i(s)}{U_i(s)} = \frac{X_i(s)}{A_i(s)} = \frac{e^{-\phi_i s}}{(1 + s\tau_i)s^2} \tag{2.5}$$

In this equation, $\tau_i$ stands for the driveline dynamics of the respective vehicle, $\phi_i$ represents the delay between the control input being generated and the time of actuator realization. The squared $s$ term (double integrator) is there for translating acceleration input to position output.

## 2.2 String Stability

The term string stability expresses the stability of the chain of vehicles applying CACC with respect to each other. In control theory, when a system is questioned whether it is stable or not, it is meaningful to talk about its individual stability with respect to different definitions of stability (BIBO stability, Lyapunov stability etc.). However, in CACC, stability of individual systems, i.e. vehicles, is no longer the utmost concern since that kind of stability can not guarantee collision-free drive dynamics. String stability, instead, introduces a new notion to the definition of stability by considering the attenuation of acceleration and velocity signals along the subsequent vehicles. This attenuation of acceleration and velocity signals may equivalently be interpreted as the decrease in the responses of vehicles to the variations of the leader vehicle's acceleration or velocity. Since CACC is aimed to be a part of the future

autonomous driving functionality, it has to ensure safety of the travellers. The measure of safety can be expressed mathematically by different types of string stability definitions. Although many of those definitions promise secure driving functionality in theory they have to be tested thoroughly under various conditions to be labeled as safe. Therefore, choosing and designing controllers that satisfy the strongest type of string stability definition will be a wiser choice and expected to be holding a better solution of the problem.

In literature, there have been different approaches to define and satisfy string stability. Feng *et. al.* [23] summarized various definitions. The most common type of string stability definition is derived by comparing the norms of successive vehicles' output signals (e.g. acceleration signals). For string stability, each and every follower vehicles' norm of acceleration signal must be less than its predecessor's. To recall, $L_p$ norm of a signal $x$ is defined as

$$\|x\|_p = \sqrt[p]{\sum_{i=1}^{n} |x_i|^p}. \tag{2.6}$$

In general, the $L_2$ and $L_\infty$ are the most preferred norms to define string stability with. Having a closer look at Equation (2.6), it is easily recognized that the $L_2$ norm is no other than square root of sum of squares, which is therefore also referred as 'Euclidean Norm'. And, the $L_\infty$ norm is maximum of a series. Thus, definition of $L_2$ norm deals with the energy of signals. Thus, $L_2$ string stability guarantees that the output signals will have less energy than the input signals. On the other hand, $L_\infty$ norm string stability considers and compares the supremum of input and output signals which means the maximum magnitude of the output signal would have to be less than the maximum of the input signal. There can be an extension made to the definition of $L_\infty$ string stability, which is to satisfy that there shall not be any overshoots in the system response. This additional condition yields a new form of string stability, namely, string stability without overshoot.

For example, in Figure 2.4, it can be seen that the acceleration signals are not attenuated towards the tail of the string of vehicles. This is a typical output of a string unstable CACC to step inputs which will cause collisions in certain scenarios. On the contrary, Figure 2.5 is a string stable example where there shall not be any collisions

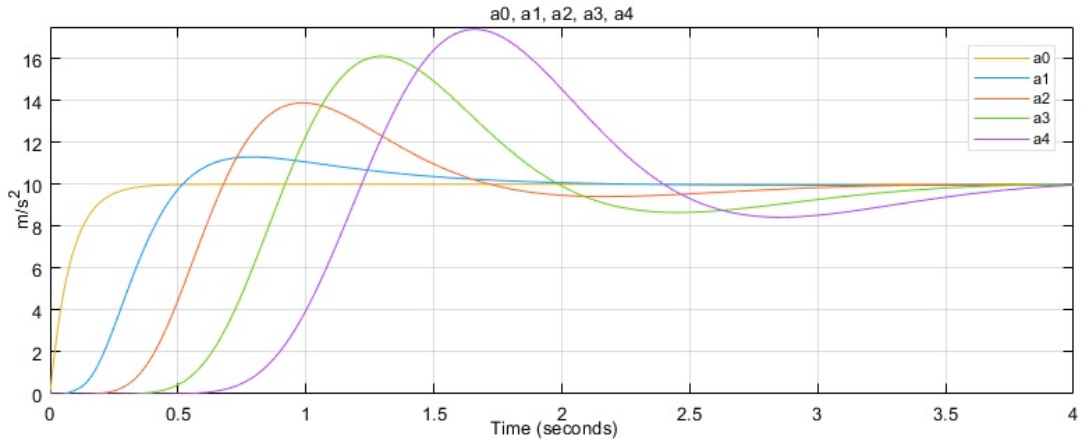


Figure 2.4: String Unstable Acceleration Signals

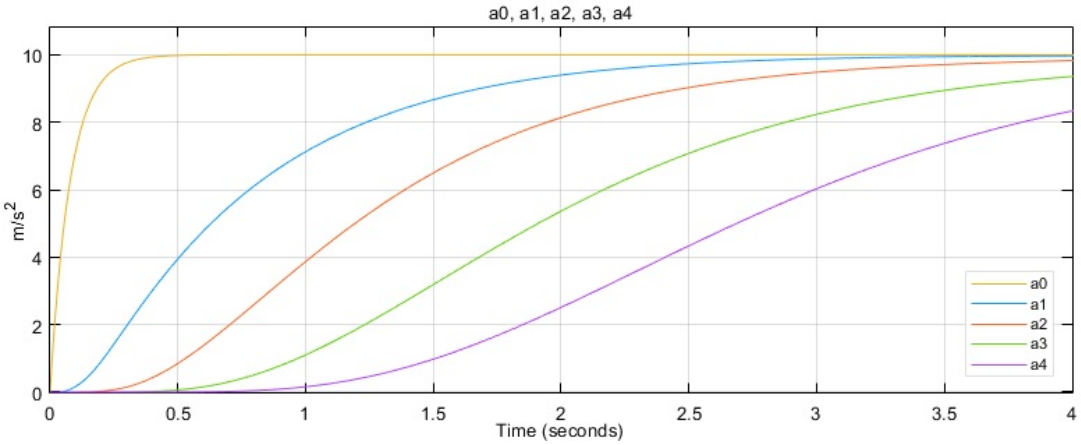


Figure 2.5: String Stable Acceleration Signals

between the vehicles due to CACC.

Mathematically, all these different definitions of string stability can be expressed with certain conditions, some being stronger than the other in terms of stability and safety measures. As will be discussed in further detail in the following sections, the one condition which will be brought attention to in this thesis will be satisfying a positive impulse response in the time domain. This will guarantee that we satisfy all string stability definitions given above.

To be able to discuss string stability we define the following so called output string stability transfer function between successive vehicles' acceleration signals. Let the output signals be denoted as

$$\mathscr{L}^{-1}\{Y_i(s)\} = y_i(t) = a_i(t). \tag{2.7}$$

Then the output string stability transfer function whose block diagram illustration was given in Figure 2.1 is

$$\Gamma_i(s) = \frac{Y_i(s)}{Y_{i-1}(s)} = \frac{G_i(s)}{G_{i-1}(s)} \frac{F_i(s) + G_{i-1}(s)C_i(s)}{1 + H_i(s)G_i(s)C_i(s)}. \tag{2.8}$$

Note that for homogeneous strings it will be reduced to the following expression by the cancellation of vehicle dynamics transfer functions.

$$\Gamma_i(s) = \frac{Y_i(s)}{Y_{i-1}(s)} = \frac{F_i(s) + G(s)C_i(s)}{1 + H_i(s)G(s)C_i(s)}. \tag{2.9}$$

Then, the following condition on $\Gamma_i$ will be sufficient to say that the CACC is strictly $L_2$ string stable [1].

$$\|\Gamma_i(j\omega)\|_\infty = \max_\omega |\Gamma_i(j\omega)| \leq 1 \tag{2.10}$$

Equivalently, Equation (2.10), in time domain, corresponds to the condition that

$$\|y_i(t)\|_{L_2} \leq \|y_{i-1}(t)\|_{L_2}, \forall i = 1, 2, ..., n \tag{2.11}$$

The Equation (2.11) is an expression of attenuation of energy in the acceleration signals of subsequent vehicles. In other words, every follower vehicle possesses less or at most equal energy than its predecessor.

Similarly, the second common type of string stability, the strict $L_\infty$ string stability, can be summarized with the following condition.

$$\|\gamma_i(t)\|_1 \leq 1 \tag{2.12}$$

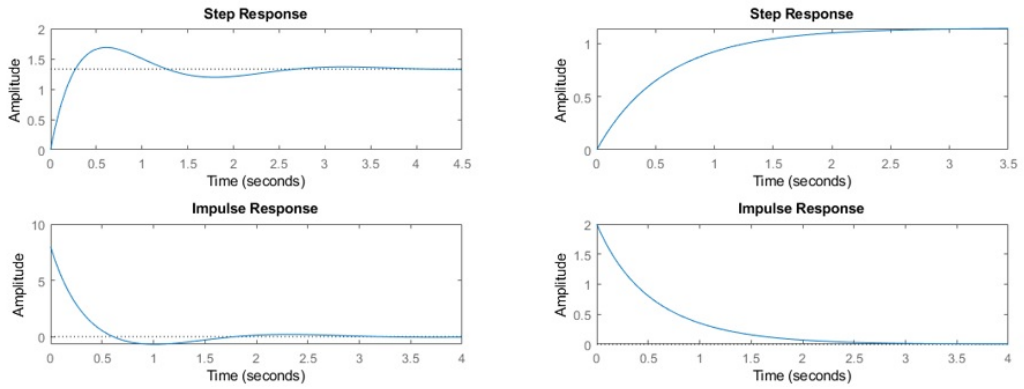


Figure 2.6: Impulse response examples with corresponding step responses

However, doing analysis on the time domain entity $\gamma_i$ is quite difficult and it can alternatively be obtained by satisfying the following two sufficient conditions at the same time.

$$\|\Gamma\|_\infty \leq 1, \gamma(t) \geq 0, \forall t \tag{2.13}$$

The effectiveness of designing CACC with positive impulse responses comes into play right at this point. Since it is known that

$$|\Gamma(0)| \leq \|\Gamma\|_\infty \leq \|\gamma\|_1. \tag{2.14}$$

Definition of Laplace transform allows us to write

$$|\Gamma(0)| = \left| \int_0^\infty \gamma(t)dt \right| \leq \int_0^\infty |\gamma(t)|dt = \|\gamma\|_1. \tag{2.15}$$

Consequently, provided that the impulse response $\gamma$ is non-negative

$$\|\Gamma\|_\infty = \|\gamma\|_1. \tag{2.16}$$

Therefore, guaranteeing a positive impulse response and having a bode plot which never goes above $0dB$ both at the same time in the CACC design guarantees a more stringent type of string stability than both $L_2$ and $L_\infty$ cases.

## 2.3 Positive Impulse Response

Impulse response, being the inverse Laplace transform of a transfer function, is a unique entity in hand to work on and manipulate through controller of choice. In

many cases, it can be used as a design parameter or a checkpoint to see whether a system will satisfy specific conditions and constraints put on its input-output relationship. In particular, having a positive impulse response will yield a step response with no undershoots and no overshoots. A pair of impulse responses featuring this property and not featuring it are shared in the Figure 2.6. This property and implication becomes useful and meaningful for a CACC since it reassures that any stepwise change in the leader vehicle's acceleration, due to either disturbances or reference point velocity changes, will be followed without any oscillations, and hence, there shall not be any collisions. It is one of the safest options for attaining string stability.

Herein, the impulse responses of the transfer functions between successive vehicles' acceleration signals will be assumed to be only consisting of exponential terms. This assumption will be laid out in detail in the following section and it will be seen with quite reasonable assumptions on the plant model and choice of controller, the impulse response of the closed loop transfer function, with predecessor acceleration input fed forward in the follower vehicle's controller structure, is going to be sum of exponentials whose coefficients and decay factors will be expressed with the constants from problem's dynamics and controller parameters.

The generic time domain expression for the impulse response of closed loop transfer function given in Equation (2.8) is

$$\gamma(t) = a_0 e^{\alpha_0} + a_1 e^{\alpha_1} + a_2 e^{\alpha_2} + a_3 e^{\alpha_3}. \tag{2.17}$$

This impulse response's coefficients and decay factors can be manipulated and tuned with the choice of controller. In [24], Laguerre presented the conditions on number of alternations of time series composed of exponential terms in detail on his paper named '*On The Theory of Numeric Equations*'. In this thesis work, we have used those derived conditions to impose them as nonlinear constraints to an optimization problem where the objective is formulated to make sure the intervehicle time gap $h$ is minimized while at the same time a safe and secure string stable CACC performance is established.

To automate robust and effective CACC design, there has to be a well defined procedure which will overcome possible difficulties that can be encountered in heterogeneous vehicle strings while at the same time guaranteeing a satisfactory longitudinal

following performance. In fact, if this procedure was to permit tuning of the dynamic response of the vehicle string, then it will be more than just a satisfactory solution. Laguerre's mathematical derivations and analysis of number of alternations of certain types of series sums [24], with reasonably valid assumptions on the model and the use scenario of the CACC design, serves this purpose.

Particularly, in his work, he has dealt with finding conditions on the coefficients and decay factors of the time series alike the one in Equation (2.17) which we are concerned with. He started by stating that the integral expression, $\Theta(z)$ is a piecewise-polynomial integrand,

$$\int_a^b e^{-zx}\Theta(z)dz = 0 \tag{2.18}$$

can be rearranged* into the form

$$e^{\alpha_0 x}f_0(x) + e^{\alpha_1 x}f_1(x) + ... + e^{\alpha_n x}f_n(x) = 0, \tag{2.19}$$

where $\alpha_i$ and $f_i$ are constants and polynomials. Then, the following coefficients were defined,

$$p_0 = a_0, \tag{2.20}$$

$$p_1 = a_0 + a_1, \tag{2.21}$$

$$p_2 = a_0 + a_1 + a_2, \tag{2.22}$$

$$....., \tag{2.23}$$

$$p_n = a_0 + a_1 + a_2 + ... + a_n. \tag{2.24}$$

Afterwards, the following integral was considered.

$$\int_{\alpha_0}^{\alpha_1} e^{-zx}p_0dz + \int_{\alpha_1}^{\alpha_2} e^{-zx}p_1dz + \int_{\alpha_2}^{\alpha_3} e^{-zx}p_2dz + ... + \int_{\alpha_n}^{\infty} e^{-zx}p_0dz = 0 \tag{2.25}$$

This integral is then transformed into

$$a_0e^{-\alpha_0 x} + a_1e^{-\alpha_1 x} + a_2e^{-\alpha_2 x} + ... + a_ne^{-\alpha_n x} = 0. \tag{2.26}$$

Replacing

$$e^{-x} = z, \tag{2.27}$$

Equation (2.26) becomes

$$a_0z^{\alpha_0} + a_1z^{\alpha_1} + a_2z^{\alpha_2} + ... + a_nz^{\alpha_n} = 0 \tag{2.28}$$

* integration by parts followed by clearing powers of x from the denominator

It is noted that the number of positive roots of Equation (2.26) is the same as the number of roots of (2.28) which lie between $0$ and $1$. Furthermore, it can be rigorously proven that the number of positive roots of Equation (2.26) is equal to the number of alternations of the series

$$\int_{\alpha_0}^{\alpha_1} p_0 dz + \int_{\alpha_1}^{\alpha_2} p_1 dz + \int_{\alpha_2}^{\alpha_3} p_2 dz + ... + \int_{\alpha_n}^{\infty} p_0 dz = 0. \tag{2.29}$$

Thus, the following proposition is made:

*Arranging* $\alpha_0, \alpha_1, \alpha_2, ..., \alpha_n$ *in increasing order, the number of positive roots of Equation* (2.26) *is no more than the number of alternations of the series*

$$p_0(\alpha_1 - \alpha_0) + p_1(\alpha_2 - \alpha_1) + ... + p_{n-1}(\alpha_n - \alpha_{n-1}) + p_n.\infty^{\dagger}. \tag{2.30}$$

This is the simplest case where both $\alpha_i$ and $a_i$ are all assumed to be real quantities. This will have an implication in positive impulse response CACC design imposing a nonlinear equality constraint which is going to be dug up in the next chapter as this proposition will be utilized and investigated.

[†] The number of alternations of the series $a + b + c + d.\infty$ is the number of variations of the terms of the sequence $a, a + b, a + b + c, d$.

# CHAPTER 3

# POSITIVE IMPULSE RESPONSE COOPERATIVE ADAPTIVE CRUISE CONTROLLER

## 3.1 Introduction

This chapter can be thought as the main body where the main outcomes of this thesis work will be shared. As it is evident that robustness and efficiency are utmost concern in CACC controller design, in this chapter it will be made clear that the approach of coming up with controllers which yield positive impulse response closed loop transfer functions between successive vehicles is one guaranteed way to achieve them. The theoretical background in the previous chapter forms the basis of our study here in this chapter. Provided that certain conditions are met in the time domain expression of a transfer function, there can be optimal solutions with positive impulse responses. The optimality measure is one of the key factors and its choice, by itself, a part of the problem which requires more and more studies to be carried on.

In short, the following sections will first develop the formulation of an optimization problem for the CACC controller parameters. Then, different cases for the optimization problem are identified and the solution of the optimization problem is discussed. As the last section of this chapter, the results obtained in simulations and the validation of string stability with satisfactory performance under a wide spectrum of circumstances will be shared and discussed.

## 3.2 Impulse Response Formulation

To formulate the impulse response between consecutive vehicles, let us reconsider the closed loop transfer function that belongs to a heterogeneous string.

$$\Gamma_i(s) = \frac{G_i(s)}{G_{i-1}(s)} \frac{F_i(s) + G_{i-1}(s)C_i(s)}{1 + H_i(s)G_i(s)C_i(s)}. \tag{3.1}$$

In the literature, for the control scheme in Figure 2.2 there have been several approaches on how to implement the feedforward path [1, 12, 14, 20]. In our formulation we are going to use so called *input signal feedforward* (ISF) as the feedforward method. Moreover, at the feedforward path we are going to assume that no communication delay exists for the formulation of our optimization problem. Hence, the feedforward transfer function becomes

$$F_i(s) = \frac{1}{H_i(s)} \tag{3.2}$$

Where

$$H_i(s) = 1 + h_i s \tag{3.3}$$

Which was explained in detail in Section 2.1. As the longitudinal vehicle dynamics transfer function we will use the aforementioned model in (2.5) with the assumption that there exists no actuator delays ($\phi_i = 0$).

The assumptions of zero delays for communication and actuation are necessary for an analytical evaluation of the vehicle-to-vehicle transfer function. Otherwise, the proposed method is not applicable even if $2^{nd}$ or $1^{st}$ order Padé approximations were to be used, and the mathematical work required for formulating an optimization problem becomes arduous and untraceable.

Finally, the controller choice is going to be a proportional-derivative controller as

$$C_i(s) = \frac{K_{p,i} + K_{d,i}s}{H_i(s)}. \tag{3.4}$$

Then Equation (3.1) becomes

$$\begin{aligned}\Gamma_i(s) &= \frac{1+\tau_{i-1}s}{1+\tau_i s}\frac{\frac{s^2(1+\tau_{i-1}s)+(K_{p,i}+K_{d,i}s)}{s^2(1+h_i s)(1+\tau_{i-1}s)}}{\frac{s^2(1+\tau_i)+(K_{p,i}+K_{d,i}s)}{s^2(1+\tau_i s)}} \\ &= \frac{1+\tau_{i-1}s}{1+\tau_i s}\frac{\big[s^2(1+\tau_{i-1}s)+(K_{p,i}+K_{d,i}s)\big](1+\tau_i s)}{(1+h_i s)(1+\tau_{i-1})\big[s^2(1+\tau_i)+(K_{p,i}+K_{d,i}s)\big]} \\ &= \frac{s^2(1+\tau_{i-1}s)+(K_{p,i}+K_{d,i}s)}{(1+h_i s)\big[s^2(1+\tau_i)+(K_{p,i}+K_{d,i}s)\big]} \\ &= \frac{\tau_{i-1}s^3+s^2+K_{d,i}s+K_{p,i}}{\tau_i h_i s^4+(\tau_i+h_i)s^3+(h_i K_{d,i}+1)s^2+(h_i K_{p,i}+K_{d,i})s+K_{p,i}} \end{aligned} \tag{3.5}$$

It must be noted that the closed loop transfer function has a $4^{th}$ order denominator. Therefore, there will be $4$ poles and they will manifest themselves as $4$ exponential terms in the impulse response.

To be able to extract the poles of the closed loop transfer function in terms of the CACC design parameters $K_{p,i}, K_{d,i}, h_i$ and driveline dynamics' constants $\tau_i$, partial fraction expansion is applied to Equation (3.5).

$$\begin{aligned}\Gamma_i(s) = &\left[\frac{(\tau_{i-1}-\tau_i)(1-K_{d,i}h_i+K_{p,i}h_i^2)}{(K_{p,i}h_i^3-K_{d,i}h_i^2+h_i-\tau_i)}\right]\frac{s^2}{\tau_i s^3+s^2+K_{d,i}s+K_{p,i}} \\ &+\left[\frac{(\tau_{i-1}-\tau_i)(K_{d,i}-K_{p,i}h_i)}{K_{p,i}h_i^3-K_{d,i}h_i^2+h_i-\tau_i}\right]\frac{s}{\tau_i s^3+s^2+K_{d,i}s+K_{p,i}} \\ &+\left[\frac{(\tau_{i-1}-\tau_i)K_{p,i}}{K_{p,i}h_i^3-K_{d,i}h_i^2+h_i-\tau_i}\right]\frac{1}{\tau_i s^3+s^2+K_{d,i}s+K_{p,i}} \\ &+\left[\frac{K_{p,i}h_i^3-K_{d,i}h_i^2+h_i-\tau_{i-1}}{K_{p,i}h_i^3-K_{d,i}h_i^2+h_i-\tau_i}\right]\frac{1}{h_i s+1}\end{aligned} \tag{3.6}$$

Equation (3.6) gives a lot of insight into the possible impulse responses of the system. It is evident that one of the poles is always introduced by the chosen spacing policy which is purely real, and the headway time constant $h_i$ determines its location on the real axis. For instance, seeking '$0$' headway time would mean trying to push that pole to '$-\infty$' which makes sense, since intuitively it would be expected that the best case scenario is supposed to be the most difficult to realize.

Next, the roots of the $3^{rd}$ order polynomial that shows up in the denominator of the closed loop transfer function are to be found symbolically.

$$D(s) = \tau_i s^3 + s^2 + K_{d,i}s + K_{p,i} = 0 \tag{3.7}$$

At this step, the cubic formula for solving any $3^{rd}$ order polynomial equation [25] was utilized. It is an interesting fact that this kind of a formula was first published by Cardano [26] in 1545. Thankfully, there are now available computation tools which can walk us through such problems [27].

Now for readability and compactness, let us introduce the following three intermediary constants which are functions of the controller parameters and the driveline dynamics constants:

$$c_{1,i} = (-27\tau_i^2 K_{d,i} + 9\tau_i K_{d,i} - 2), \tag{3.8}$$

$$c_{2,i} = (3\tau_i K_{d,i} - 1), \tag{3.9}$$

$$c_{3,i} = \sqrt[3]{(\sqrt{(c_{1,i}^2 + 4c_{2,i}^3)} + c_{1,i})}. \tag{3.10}$$

The roots are then given as

$$s_{1,i} = \frac{c_{3,i}}{3\sqrt[3]{2}\tau_i} - \frac{\sqrt[3]{2}c_{2,i}}{3\tau_i c_{3,i}} - \frac{1}{3\tau_i} \tag{3.11}$$

$$s_{2,i} = \frac{(1+i\sqrt{3})c_{2,i}}{3\sqrt[3]{4}\tau_i c_{3,i}} - \frac{(1-i\sqrt{3})c_{3,i}}{6\sqrt[3]{2}\tau_i} - \frac{1}{3\tau_i} \tag{3.12}$$

$$s_{3,i} = \frac{(1-i\sqrt{3})c_{2,i}}{3\sqrt[3]{4}\tau_i c_{3,i}} - \frac{(1+i\sqrt{3})c_{3,i}}{6\sqrt[3]{2}\tau_i} - \frac{1}{3\tau_i}. \tag{3.13}$$

Then Equation (3.6) can be rewritten as

$$\begin{aligned}\Gamma_i(s) = &\left[\frac{(\tau_{i-1}-\tau_i)(1-K_{d,i}h_i+K_{p,i}h_i^2)}{(K_{p,i}h_i^3 - K_{d,i}h_i^2 + h_i - \tau_i)}\right]\frac{s^2}{(s+s_{1,i})(s+s_{2,i})(s+s_{3,i})} \\ &+ \left[\frac{(\tau_{i-1}-\tau_i)(K_{d,i}-K_{p,i}h_i)}{K_{p,i}h_i^3 - K_{d,i}h_i^2 + h_i - \tau_i}\right]\frac{s}{(s+s_{1,i})(s+s_{2,i})(s+s_{3,i})} \\ &+ \left[\frac{(\tau_{i-1}-\tau_i)K_{p,i}}{K_{p,i}h_i^3 - K_{d,i}h_i^2 + h_i - \tau_i}\right]\frac{1}{(s+s_{1,i})(s+s_{2,i})(s+s_{3,i})} \\ &+ \left[\frac{K_{p,i}h_i^3 - K_{d,i}h_i^2 + h_i - \tau_{i-1}}{K_{p,i}h_i^3 - K_{d,i}h_i^2 + h_i - \tau_i}\right]\frac{1}{h_i s + 1}.\end{aligned} \tag{3.14}$$

Now the only step left before obtaining the time domain expression of the impulse response is to take inverse Laplace transform of $\Gamma_i(s)$. Before proceeding with inverse Laplace transform, we note that the roots of Equation (3.7) are composed of one complex-conjugate pair ($s_{2,i} = s_{3,i}^*$) and a single real one ($s_{1,i}$). Here, if we impose the necessary conditions on the conjugate pair poles to equate their complex part to zero,

then we can get an easier inverse Laplace transform expression. It will also be the one that we would like to have for being able to examine with the given proposition in section 2.3. That is, the resultant time domain expression will be in the same form with Equation (2.26). To derive those conditions to be imposed, we consider Equations (3.12),(3.13) and equate the imaginary parts to zero.

$$\Im(s_{2,i}) = -\Im(s_{3,i}) = 0 \tag{3.15}$$

This yields

$$c_{3,i} = \sqrt{-\sqrt[3]{4}c_{2,i}}. \tag{3.16}$$

Therefore,

$$\sqrt[3]{4}c_{2,i} + c_{3,i}^2 = 0 \tag{3.17}$$

And since we cannot tolerate a negative square root term,

$$c_{2,i} = 3\tau_i K_{d,i} - 1 \leq 0. \tag{3.18}$$

Again for simplicity and to keep the terms traceable we define the following intermediary constants:

$$k_{1,i} = \left[\frac{(\tau_{i-1} - \tau_i)(1 - K_{d,i}h_i + K_{p,i}h_i^2)}{(K_{p,i}h_i^3 - K_{d,i}h_i^2 + h_i - \tau_i)}\right], \tag{3.19}$$

$$k_{2,i} = \left[\frac{(\tau_{i-1} - \tau_i)(K_{d,i} - K_{p,i}h_i)}{K_{p,i}h_i^3 - K_{d,i}h_i^2 + h_i - \tau_i}\right], \tag{3.20}$$

$$k_{3,i} = \left[\frac{(\tau_{i-1} - \tau_i)K_{p,i}}{K_{p,i}h_i^3 - K_{d,i}h_i^2 + h_i - \tau_i}\right], \tag{3.21}$$

$$k_{4,i} = \left[\frac{K_{p,i}h_i^3 - K_{d,i}h_i^2 + h_i - \tau_{i-1}}{K_{p,i}h_i^3 - K_{d,i}h_i^2 + h_i - \tau_i}\right]. \tag{3.22}$$

Hence,

$$\mathscr{L}^{-1}\{\Gamma_i(s)\} = \mathscr{L}^{-1}\left\{\frac{k_{1,i}s^2 + k_{2,i}s + k_{3,i}}{D(s)}\right\} + \mathscr{L}^{-1}\left\{\frac{k_{4,i}}{h_i s + 1}\right\}. \tag{3.23}$$

Reiterating that $s_{2,i} = s_{3,i}$, $\gamma_i$ becomes

$$\gamma_i(t) = \left[\frac{e^{s_{2,i}t}(k_{1,i}s_{2,i}^2 - 2k_{1,i}s_{1,i}s_{2,i})}{(s_{1,i} - s_{2,i})^2} + \frac{k_{1,i}s_{1,i}^2 e^{s_{1,i}t}}{(s_{1,i} - s_{2,i})^2} + \frac{(k_{1,i}s_{2,i}^2 te^{s_{2,i}t})}{(s_{1,i} - s_{2,i})}\right] + \left[\frac{k_{2,i}s_{1,i}e^{s_{2,i}t}}{(s_{1,i} - s_{2,i})^2} - \frac{k_{2,i}s_{1,i}e^{s_{1,i}t}}{(s_{1,i} - s_{2,i})^2} - \frac{k_{2,i}s_{2,i}te^{s_{2,i}t}}{(s_{1,i} - s_{2,i})}\right] + \left[\frac{k_{3,i}e^{s_{1,i}t}}{(s_{1,i} - s_{2,i})^2} - \frac{k_{3,i}e^{s_{2,i}t}}{(s_{1,i} - s_{2,i})^2} + \frac{k_{3,i}te^{s_{2,i}t}}{(s_{1,i} - s_{2,i})}\right] + \left[\frac{k_{4,i}e^{-t/h_i}}{h_i}\right]. \quad (3.24)$$

Rearranging the terms we get

$$\gamma_i(t) = \frac{k_{4,i}}{h_i}e^{-t/h_i} + \left[\frac{k_{1,i}s_{1,i}^2 - k_{2,i}s_{1,i} + k_{3,i}}{(s_{1,i} - s_{2,i})^2}\right]e^{s_{1,i}t} + \left[\frac{k_{1,i}s_{2,i}^2 - 2k_{1,i}s_{1,i}s_{2,i} + k_{2,i}s_{1,i} - k_{3,i}}{(s_{1,i} - s_{2,i})^2}\right]e^{s_{2,i}t} + \left[\frac{k_{1,i}s_{2,i}^2 - k_{2,i}s_{2,i} + k_{3,i}}{(s_{1,i} - s_{2,i})}\right]te^{s_{2,i}t}. \quad (3.25)$$

In this equation, Equation (3.25), it is going to be assumed that if the coefficient of the $te^t$ term can be forced to go to $0$ by the choice of design parameters, then the remaining part will resemble Equation (2.26). Thereafter, the proposition given in Section 2.3 for Equation (2.30) can be exploited. Hence, we want to impose

$$\left[\frac{k_{1,i}s_{2,i}^2 - k_{2,i}s_{2,i} + k_{3,i}}{(s_{1,i} - s_{2,i})}\right] = 0. \quad (3.26)$$

We see benefit in underlining a fact here, that is, we are going to try to achieve two equations via optimization, Equations (3.15) and (3.26), in order to be able to use the proposition coming from Laguerre's mathematical work [24]. The crucial point to be remembered is that Laguerre's proposition facilitates arriving at the sufficient conditions. Therefore, even if those two constraints of the optimization process were to be violated at the end, that does not necessarily mean the ultimate goal of attaining positive impulse responses has failed. Rather, the resultant vehicle-to-vehicle transfer function has to be checked to see whether it possesses a positive impulse response or not. In other words, trying to push the solver to converge to a guaranteed region with

potentially small violations of (3.26) by aiming to arrive at sufficient conditions may quite likely be a successful way to achieve a positive impulse response.

After this point, we need to examine different scenarios where modes of the system are arranged in increasing order. There are 6 different possibilities in the arrangement of the modes of the system, which are given as

$$s_{2,i} < s_{1,i} < \frac{-1}{h_i} < 0, \tag{3.27}$$

$$s_{1,i} < s_{2,i} < \frac{-1}{h_i} < 0, \tag{3.28}$$

$$s_{2,i} < \frac{-1}{h_i} < s_{1,i} < 0, \tag{3.29}$$

$$s_{1,i} < \frac{-1}{h_i} < s_{2,i} < 0, \tag{3.30}$$

$$\frac{-1}{h_i} < s_{2,i} < s_{1,i} < 0, \tag{3.31}$$

$$\frac{-1}{h_i} < s_{1,i} < s_{2,i} < 0. \tag{3.32}$$

For each of these cases, the series sum given in Equation (2.30) has to be evaluated and examined. Fulfilling the conditions stated in the aforementioned proposition, a positive impulse response can be attained with the resultant controller. On how to develop and introduce those conditions to an optimization problem whose outputs are the design parameters, the next section will lay down the road map and give insights.

## 3.3 The Optimization Problem

An optimization problem is formed to seek the best possible solution for a set of unknown parameters where the best solution is assumed to be the one that minimizes a certain cost function which is in general a function of the parameter set to be found. While doing this, the problem may or may not have linear and nonlinear or, equality or inequality constraints on the parameter set. This type of optimization problems are also called nonlinear programming problems where the solver finds the minimum of

a function specified as

$$\min_{\mathbf{x}} f(\mathbf{x}) \text{ subject to } \begin{cases} c(\mathbf{x}) \leq 0 \\ c_{eq}(\mathbf{x}) = 0 \\ A\mathbf{x} \leq b \\ A_{eq}\mathbf{x} = b_{eq} \\ lb \leq \mathbf{x} \leq ub. \end{cases} \tag{3.33}$$

In Equation (3.33), $\mathbf{x}$ is the vector of unknowns, $c$ and $c_{eq}$ are used to express nonlinear inequality and equality constraints respectively. Similarly, $A$, $b$, $A_{eq}$ and $b_{eq}$ are used to express linear ones. Lastly, $lb$ and $ub$ correspond to specified upper and lower bounds for the parameters to be found in $\mathbf{x}$.

In our optimization problem for the CACC controller design, the vector $\mathbf{x}$ is determined by the choice of controller gains for every individual vehicle in Equation (3.4) and the headway time constant in Equation (3.3) as

$$\mathbf{x}_i = \begin{bmatrix} x_{1,i} \\ x_{2,i} \\ x_{3,i} \end{bmatrix} = \begin{bmatrix} K_{p,i} \\ K_{d,i} \\ h_i \end{bmatrix} \tag{3.34}$$

With the given formulation in above Equation (3.33), the next task is to translate positive impulse response CACC problem, which was thoroughly discussed in the previous section 3.2, into an optimization problem in the same form and seek robust and efficient solutions. For this purpose, we have to examine 6 different cases of order of poles as given in Equations (3.27)-(3.32). In the following subsections, we will be defining the necessary constraints for formulating the optimization problem for all these different arrangements of poles.

Furthermore, we would like to note that in all these cases there will be three common constraints, two of which come from equating the imaginary parts of the poles as given in Equation (3.15), and the other comes from equating $te^{s_{2,i}t}$ term's coefficient to zero. Since these three always remain the same in all 6 cases, we think that it fits mentioning them once before detailing all the definitions in the upcoming subsections.

Firstly, equating the imaginary parts to zero yields the nonlinear equality constraint shown in Equation (3.17), and the linear inequality constraint shown in Equation

(3.18) which results in

$$A\mathbf{x} = [0\ 3\tau_{i-1}\ 0] \begin{bmatrix} K_{p,i} \\ K_{d,i} \\ h_i \end{bmatrix} \leq b, b = 1. \tag{3.35}$$

Secondly, looking at Equation (3.25), the following coefficient term is equated to zero, yielding another nonlinear equality constraint.

$$\left[ \frac{k_{1,i}s_{2,i}^2 - k_{2,i}s_{2,i} + k_{3,i}}{(s_{1,i} - s_{2,i})} \right] = 0 \tag{3.36}$$

Which is equivalent to

$$\left[ k_{1,i}s_{2,i}^2 - k_{2,i}s_{2,i} + k_{3,i} \right] = 0. \tag{3.37}$$

Finally, the derived constants $p_{j,i}$ in Equation (2.30) for guaranteeing positive impulse response which were given as

$$p_{0,i} = a_{0,i}, \tag{3.38}$$

$$p_{1,i} = a_{0,i} + a_{1,i}, \tag{3.39}$$

$$p_{2,i} = a_{0,i} + a_{1,i} + a_{2,i} \tag{3.40}$$

are all going to be defined in the same way. Nevertheless, the exponential coefficients $a_{j,i}$ are going to be assigned differently. Moreover, using the proposition made in Section 2.3 with Equation (2.30), the following three inequalities are introduced to the optimization problem as nonlinear constraints.

$$p_{0,i}(\alpha_{1,i} - \alpha_{0,i}) \geq 0 \tag{3.41}$$

$$p_{1,i}(\alpha_{2,i} - \alpha_{1,i}) + p_{0,i}(\alpha_{1,i} - \alpha_{0,i}) \geq 0 \tag{3.42}$$

$$p_{2,i} \geq 0 \tag{3.43}$$

So the Equations (3.41), (3.42), and (3.43) are going to be common nonlinear inequality constraints but their content will be differing in every case according to ordering of poles.

To sum up, these three Equations, (3.17),(3.35), and (3.37), apply for all optimization problem formulations in the following subsections. The remainder, i.e. 3 inequalities coming from orders of poles and 3 other inequalities coming from alternating

series sum proposition, of each case's constraints formulation will be elaborated in the subsections below.

The formulated optimization problem was solved in MATLAB using '*fmincon*' function. And as for the cost function, the simplest approach is to push the closest pole to the imaginary axis, namely $\alpha_{0,i}$, as far to the left as possible. In addition, minimizing $h_i$ would also be meaningful in the sense that it is a straightforward measure of the main goals of CACC at the end of the day, fuel efficiency and traffic throughput.

### 3.3.1 Case 1

In the first case, in decreasing order the poles are $-1/h_i$, $s_{1,i}$, and $s_{2,i}$, resulting in the corresponding decay factors in exponential terms being arranged in increasing order. Recalling the form mentioned in Equation (2.17), it is noted that

$$a_{0,i} = \frac{k_{4,i}}{h_i}, \tag{3.44}$$

$$a_{1,i} = \left[\frac{k_{1,i}s_{1,i}^2 - k_{2,i}s_{1,i} + k_{3,i}}{(s_{1,i} - s_{2,i})^2}\right], \tag{3.45}$$

$$a_{2,i} = \left[\frac{k_{1,i}s_{2,i}^2 - 2k_{1,i}s_{1,i}s_{2,i} + k_{2,i}s_{1,i} - k_{3,i}}{(s_{1,i} - s_{2,i})^2}\right]. \tag{3.46}$$

And

$$\alpha_{0,i} = \frac{1}{h_i}, \tag{3.47}$$

$$\alpha_{1,i} = -s_{1,i}, \tag{3.48}$$

$$\alpha_{2,i} = -s_{2,i}. \tag{3.49}$$

As a consequence of being arranged in increasing order, three inequalities follow

$$-\alpha_{0,i} = \frac{-1}{h_i} \leq 0, \tag{3.50}$$

$$\alpha_{0,i} - \alpha_{1,i} = -\frac{-1}{h_i} + s_{1,i} \leq 0, \tag{3.51}$$

$$\alpha_{1,i} - \alpha_{2,i} = -s_{1,i} + s_{2,i} \leq 0. \tag{3.52}$$

The latter two of these three inequalities are going to be introduced as nonlinear inequality constraints to the optimization problem. The first one can be imposed by simply allowing only non-negative $h_i$ values.

Hence, Equations (3.41)-(3.43), (3.51), (3.52) define $c$ in Equation (3.33) for the first case.

### 3.3.2 Case 2

The second case is very similar to the first. The only difference is that orders of $s_{1,i}$ and $s_{2,i}$ are switched. Hence,

$$a_{0,i} = \frac{k_{4,i}}{h_i}, \tag{3.53}$$

$$a_{1,i} = \left[ \frac{k_{1,i}s_{2,i}^2 - 2k_{1,i}s_{1,i}s_{2,i} + k_{2,i}s_{1,i} - k_{3,i}}{(s_{1,i} - s_{2,i})^2} \right], \tag{3.54}$$

$$a_{2,i} = \left[ \frac{k_{1,i}s_{1,i}^2 - k_{2,i}s_{1,i} + k_{3,i}}{(s_{1,i} - s_{2,i})^2} \right]. \tag{3.55}$$

And

$$\alpha_{0,i} = \frac{1}{h_i}, \tag{3.56}$$

$$\alpha_{1,i} = -s_{2,i}, \tag{3.57}$$

$$\alpha_{2,i} = -s_{1,i}. \tag{3.58}$$

Then the three inequalities due to the order of poles are

$$-\alpha_{0,i} = \frac{-1}{h_i} \leq 0, \tag{3.59}$$

$$\alpha_{0,i} - \alpha_{1,i} = \frac{1}{h_i} + s_{2,i} \leq 0, \tag{3.60}$$

$$\alpha_{1,i} - \alpha_{2,i} = -s_{2,i} + s_{1,i} \leq 0. \tag{3.61}$$

Similar to the first case, the latter two of these three inequalities are going to be expressed in $c$ of the nonlinear optimization constraints. Once again, the first one can be achieved easily by setting the lower bound of $h_i$ equal to zero.

As mentioned previously, the inequalities coming from the alternating series sum proposition are all going to be the same in closed form. Hence, Equations (3.41)-(3.43), (3.60), (3.61) are going to constitute the nonlinear inequality constraints for the second case.

### 3.3.3 Case 3

In the third case, in decreasing order the poles are $s_{1,i}$, $-1/h_i$, and $s_{2,i}$. And the constants in the impulse response expression are defined as

$$a_{0,i} = \left[\frac{k_{1,i}s_{1,i}^2 - k_{2,i}s_{1,i} + k_{3,i}}{(s_{1,i} - s_{2,i})^2}\right], \tag{3.62}$$

$$a_{1,i} = \frac{k_{4,i}}{h_i}, \tag{3.63}$$

$$a_{2,i} = \left[\frac{k_{1,i}s_{2,i}^2 - 2k_{1,i}s_{1,i}s_{2,i} + k_{2,i}s_{1,i} - k_{3,i}}{(s_{1,i} - s_{2,i})^2}\right]. \tag{3.64}$$

And

$$\alpha_{0,i} = -s_{1,i}, \tag{3.65}$$

$$\alpha_{1,i} = \frac{1}{h_i}, \tag{3.66}$$

$$\alpha_{2,i} = -s_{2,i}. \tag{3.67}$$

Three inequalities coming from ordering of poles are then given as

$$-\alpha_{0,i} = s_{1,i} \leq 0, \tag{3.68}$$

$$\alpha_{0,i} - \alpha_{1,i} = -s_{1,i} - \frac{1}{h_i} \leq 0, \tag{3.69}$$

$$\alpha_{1,i} - \alpha_{2,i} = \frac{1}{h_i} + s_{2,i} \leq 0. \tag{3.70}$$

Since this time none of these three inequalities present themselves as non-negativity of $h_i$, it must be remarked that 3 separate nonlinear inequality constraints have to be defined. As a result, Equations (3.41)-(3.43), (3.68), (3.69),(3.70) will show up as nonlinear inequality constraints in the optimization process.

### 3.3.4 Case 4

The fourth case resembles the third, in that, the pole introduced by the inter-vehicle spacing policy constant $h_i$ is still in between the other two poles existent due to the problem dynamics, except that their order is switched. In decreasing order we have,

$s_{2,i}$, $-1/h_i$, and $s_{1,i}$. Then,

$$a_{0,i} = \left[\frac{k_{1,i}s_{2,i}^2 - 2k_{1,i}s_{1,i}s_{2,i} + k_{2,i}s_{1,i} - k_{3,i}}{(s_{1,i} - s_{2,i})^2}\right], \tag{3.71}$$

$$a_{1,i} = \frac{k_{4,i}}{h_i}, \tag{3.72}$$

$$a_{2,i} = \left[\frac{k_{1,i}s_{1,i}^2 - k_{2,i}s_{1,i} + k_{3,i}}{(s_{1,i} - s_{2,i})^2}\right]. \tag{3.73}$$

And

$$\alpha_{0,i} = -s_{2,i}, \tag{3.74}$$

$$\alpha_{1,i} = \frac{1}{h_i}, \tag{3.75}$$

$$\alpha_{2,i} = -s_{1,i}. \tag{3.76}$$

The Equation (3.30) yields

$$-\alpha_{0,i} = s_{2,i} \leq 0, \tag{3.77}$$

$$\alpha_{0,i} - \alpha_{1,i} = -s_{2,i} - \frac{1}{h_i} \leq 0, \tag{3.78}$$

$$\alpha_{1,i} - \alpha_{2,i} = \frac{1}{h_i} + s_{1,i} \leq 0. \tag{3.79}$$

Therefore, (3.41)-(3.43), (3.77), (3.78),(3.79) are nonlinear inequality constraints in the fourth case of optimization problem.

### 3.3.5 Case 5

The fifth case assumes that the pole coming from headway time constant is the farthest away from the imaginary axis. In decreasing order $s_{1,i}$, $s_{2,i}$, and $-1/h_i$. Meaning that

$$a_{0,i} = \left[\frac{k_{1,i}s_{1,i}^2 - k_{2,i}s_{1,i} + k_{3,i}}{(s_{1,i} - s_{2,i})^2}\right], \tag{3.80}$$

$$a_{1,i} = \left[\frac{k_{1,i}s_{2,i}^2 - 2k_{1,i}s_{1,i}s_{2,i} + k_{2,i}s_{1,i} - k_{3,i}}{(s_{1,i} - s_{2,i})^2}\right], \tag{3.81}$$

$$a_{2,i} = \frac{k_{4,i}}{h_i}. \tag{3.82}$$

And

$$\alpha_{0,i} = -s_{1,i}, \tag{3.83}$$

$$\alpha_{1,i} = -s_{2,i}, \tag{3.84}$$

$$\alpha_{2,i} = \frac{1}{h_i}. \tag{3.85}$$

Following the Equation (3.31), the following three inequalities are derived

$$-\alpha_{0,i} = s_{1,i} \leq 0, \tag{3.86}$$

$$\alpha_{0,i} - \alpha_{1,i} = -s_{1,i} + s_{2,i} \leq 0, \tag{3.87}$$

$$\alpha_{1,i} - \alpha_{2,i} = -s_{2,i} - \frac{1}{h_i} \leq 0. \tag{3.88}$$

Equations (3.41)-(3.43), (3.86), (3.87),(3.88) define the nonlinear inequality constraints for the fifth case.

### 3.3.6 Case 6

The sixth and the fifth are much alike cases. Orders of $s_{2,i}$ and $s_{1,i}$ are changed. Hence,

$$a_{0,i} = \left[ \frac{k_{1,i}s_{2,i}^2 - 2k_{1,i}s_{1,i}s_{2,i} + k_{2,i}s_{1,i} - k_{3,i}}{(s_{1,i} - s_{2,i})^2} \right], \tag{3.89}$$

$$a_{1,i} = \left[ \frac{k_{1,i}s_{1,i}^2 - k_{2,i}s_{1,i} + k_{3,i}}{(s_{1,i} - s_{2,i})^2} \right], \tag{3.90}$$

$$a_{2,i} = \frac{k_{4,i}}{h_i}. \tag{3.91}$$

And

$$\alpha_{0,i} = -s_{2,i}, \tag{3.92}$$

$$\alpha_{1,i} = -s_{1,i}, \tag{3.93}$$

$$\alpha_{2,i} = \frac{1}{h_i}. \tag{3.94}$$

The three inequalities coming from the ordering are given as

$$-\alpha_{0,i} = s_{2,i} \leq 0, \tag{3.95}$$

$$\alpha_{0,i} - \alpha_{1,i} = -s_{2,i} + s_{1,i} \leq 0, \tag{3.96}$$

$$\alpha_{1,i} - \alpha_{2,i} = -s_{1,i} - \frac{1}{h_i} \leq 0. \tag{3.97}$$

6 inequality constraints are defined for the last case with Equations (3.41)-(3.43), (3.95), (3.96),(3.97).

# CHAPTER 4

## SIMULATION AND VERIFICATION OF STRING STABILITY

In this chapter, we are going to present the simulation results of our studies. For simulation purposes, MATLAB and Simulink are used. From individual vehicle model to whole string of vehicles in CACC scheme, all blocks are designed in Simulink environment according to the generic formula for heterogeneous CACC closed loop transfer function given in Equation (3.1) and simulated with the outputs of the aforementioned MATLAB script.

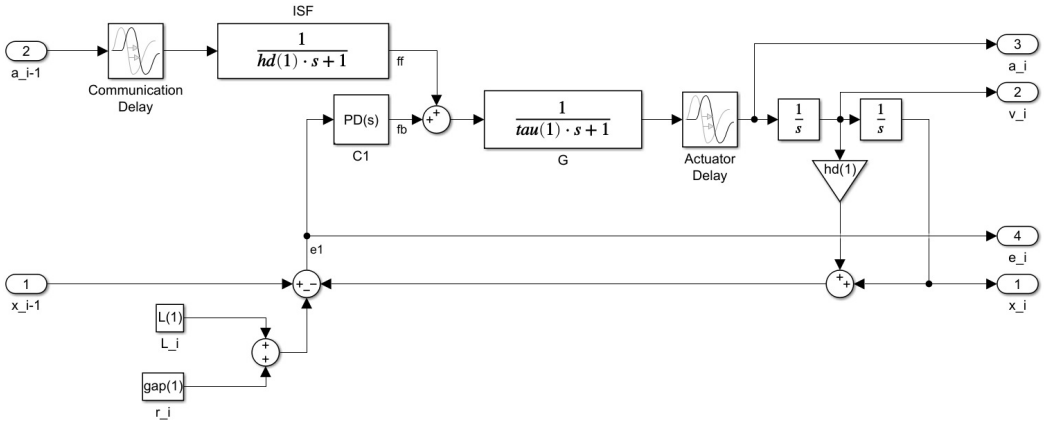


Figure 4.1: Representation of CACC in Simulink

In Figure 4.1, the Simulink model representing the translation between successive vehicles' acceleration signals is given. This Simulink block takes the predecessor vehicle's position and acceleration as input signals and produces the $i^{th}$ vehicle's acceleration, velocity, position, and positional distance keeping error signals as outputs, as shown in Figure 4.2. This block practically can be reused for arbitrarily many vehicles in forming a string. Individual vehicle parameters can be managed within

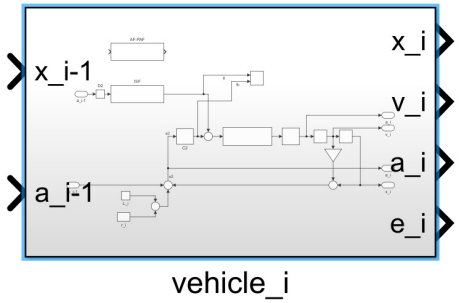


Figure 4.2: Reusable Vehicle Block Applying CACC

the blocks and assigned separately making it optional to simulate homogeneous or heterogeneous strings. Representation of a string of five consisting of four followers and a leader vehicle in Simulink environment is given in Figure 4.3. This model is used to simulate all synthesized controllers and for the comparison of results to be shared in this section.

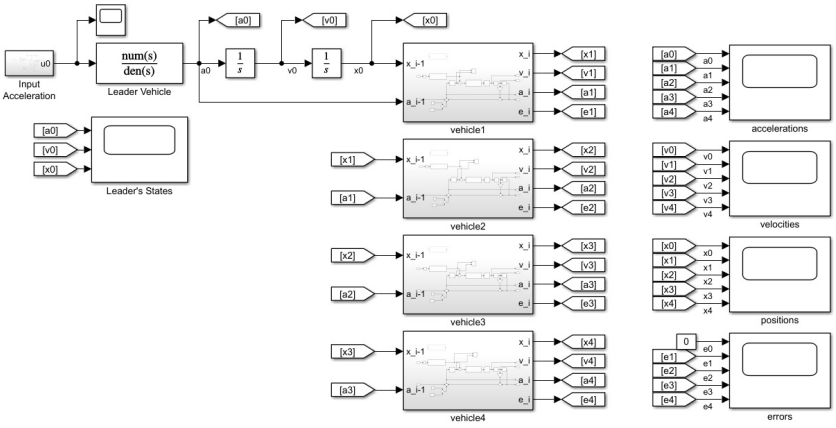


Figure 4.3: CACC Simulation Model

At this point, it must be recalled that zero communication and actuator delays were assumed in the impulse response formulation section 3.2. In this section, all results are obtained with synthesized controllers according to that assumption. However, it will be seen that even after solving the formed optimization problem with zero delays assumption the resultant controller and headway time constant parameters are capable of dealing with nonzero delays. Moreover, in all cases and simulations, the

cost function in Equation (3.33) will be defined as

$$\min_{x} f(x) = h_i - \alpha_{0,i} = x_{3,i} + \alpha_{0,i}. \tag{4.1}$$

This choice of cost function is intuitive in the sense that it both tries to push the closest pole to the imaginary axis as far as possible, making the system response as quick as possible, and minimizes the headway time as much as possible which is a direct measure of efficiency in CACC.

Within this chapter, subsequently, we will start by defining suitable test inputs to be given to the system. Secondly, we will propose and discuss the use of time-domain impulse response function based optimal CACC controller design via simulations of various driveline dynamics constants found in the literature to prove itself as an acceptable method. Then, we will investigate the effects of nonzero delays by fixing other parameters and see that they have to be limited for string stability. Therein, increasing the constant time gap between vehicles the maximum allowable delays will be evaluated and compared.

As a last note, Jhayyish and Schmidt [14] briefly went through the existing values in the literature, and adopted that

$$0.1 \leq \tau_i \leq 0.8, \quad 0.02 \leq \phi_i \leq 0.25, \quad 0.02 \leq \theta_i \leq 0.2. \tag{4.2}$$

We will use these reference values as a guide to make realistic simulations.

## 4.1 Defining The Test Input Signals

To begin with, several types of motion scenarios are defined and tested in simulation environment. One of them is constant jerk signal. In other words, the actuator of the leader vehicle produces an acceleration signal with constant slope, yielding a wave like velocity behaviour first speeding up and then slowing down periodically. In Figure 4.4, this hypothetical example acceleration signal along with the resultant velocity and position signals are given. The second example signal is much more likely to happen in a real-life traffic scenario where the leader accelerates for a period of time to a certain speed and then decelerates down to zero velocity to stop. In Figure 4.6, such a signal triad is given. The last example is somewhat similar to the previous one except for the velocity reached after acceleration is kept for a specific time interval while possessing zero acceleration and then decelerated to zero velocity. One such periodic signal pairing is given in Figure 4.5. With these three types of inputs, we are going to simulate a string of five vehicles for different investigations.

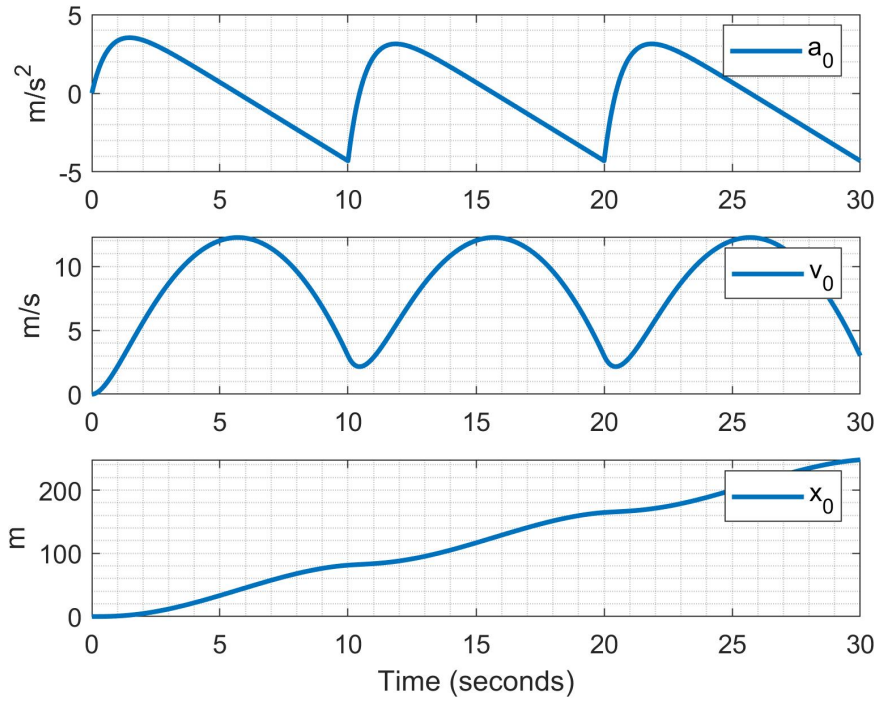


Figure 4.4: Leader vehicle's states in response to constant jerk

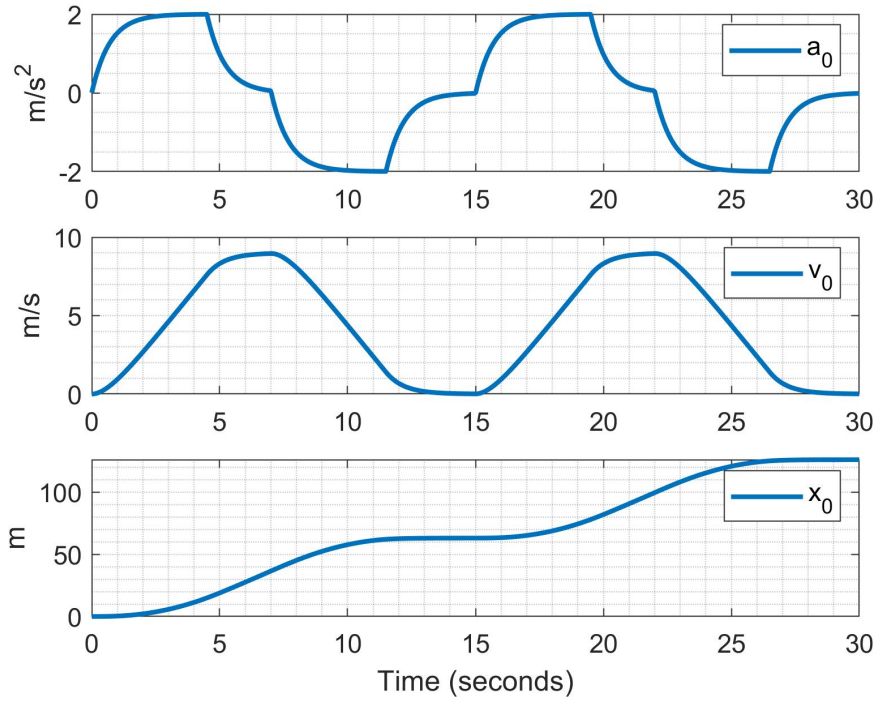


Figure 4.5: Response to acceleration-deceleration type input

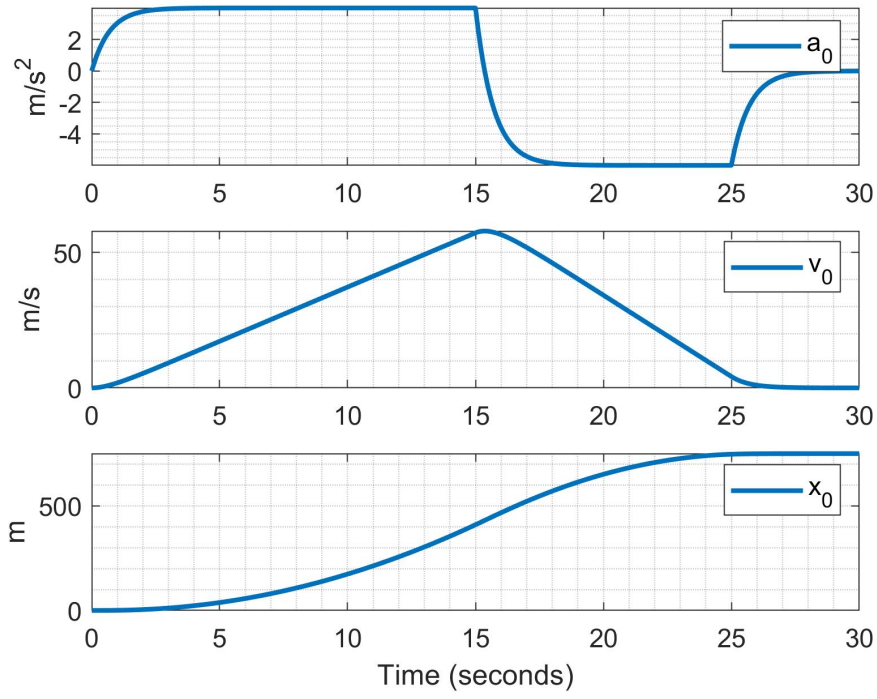


Figure 4.6: Input signal simulating acceleration and then braking to stop

## 4.2 Validation With Different Sets of Driveline Parameters

The first type of tests will be for understanding how the change in driveline dynamics affects the controller synthesis process. At the end of this section, a reasonable confidence in the developed optimization based controller design method will be gained by witnessing that it can manage to find parameters yielding strict $L_\infty$ string stability with positive impulse responses for the recognized range of driveline dynamics constant values in Equation (4.2).

First, let us consider a homogeneous string of vehicles without any delays. In a sense, it can be considered as the simplest case of CACC. The parameters to be simulated are as given in Table 4.1. The resulting controllers in case of homogeneous strings will be identical. This is clearly noted in pole-zero maps of $\Gamma_i$ transfer functions in Figures 4.7 to 4.12. Also, it must be noted that due to the cancellation in Equation (2.9), the system exhibits only a single pole.

In these simulations, another valuable thing to take note of is that the positions of resulting poles. This tells us a lot about which of the cases are more likely to yield faster responses for CACC controller design. What we noticed in our simulations is that, although the speed of responses of vehicles for each case may differ slightly with changing driveline dynamics constants, there is a trend in the speed of resultant controllers' when compared with respect to different cases. For instance, in the simulations for Table 4.1, cases 3 and 6 sticks out as the fastest ones, and the same behaviour was found in simulations for doubled and quadrupled values of $\tau_i$. Some of the plots of positive impulse response functions attained in such simulations are given in Figures 4.13 and 4.14.

| $i$ | $\theta_i$ | $\phi_i$ | $\tau_i$ |
|---|---|---|---|
| $\forall i$ | 0 | 0 | 0.16 |

Table 4.1: Zero delay homogeneous string parameter set

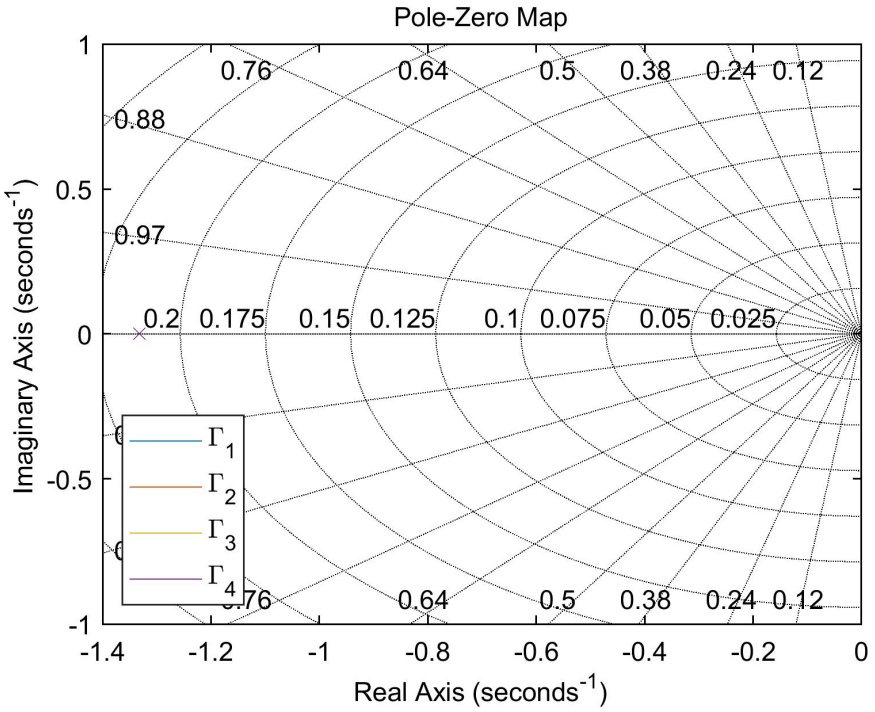


Figure 4.7: Homogeneous string $\tau_i = 0.16$, pole-zero maps of $\Gamma_i$ in case 1

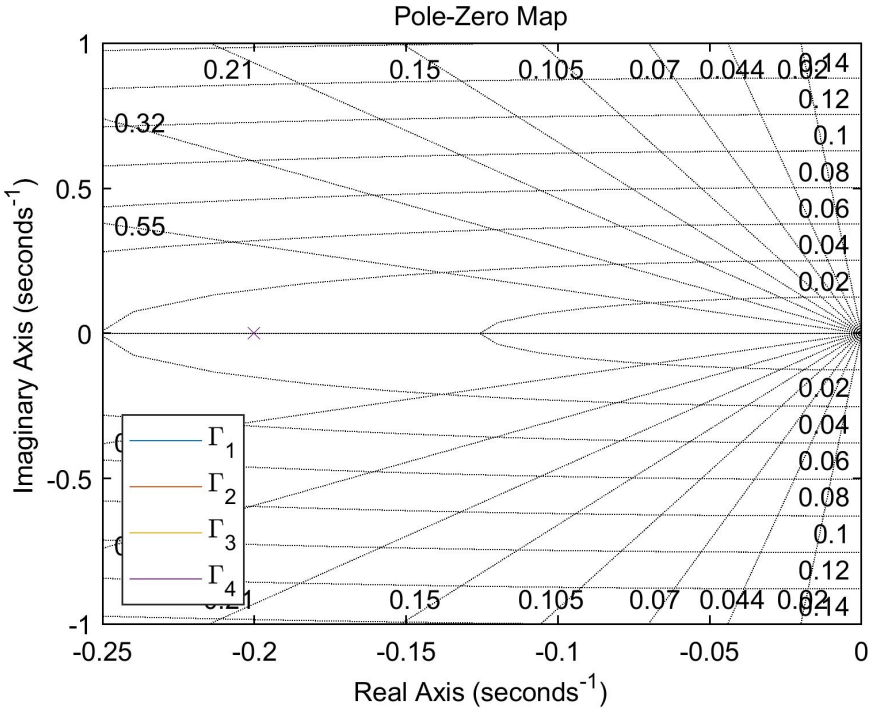


Figure 4.8: Case 2

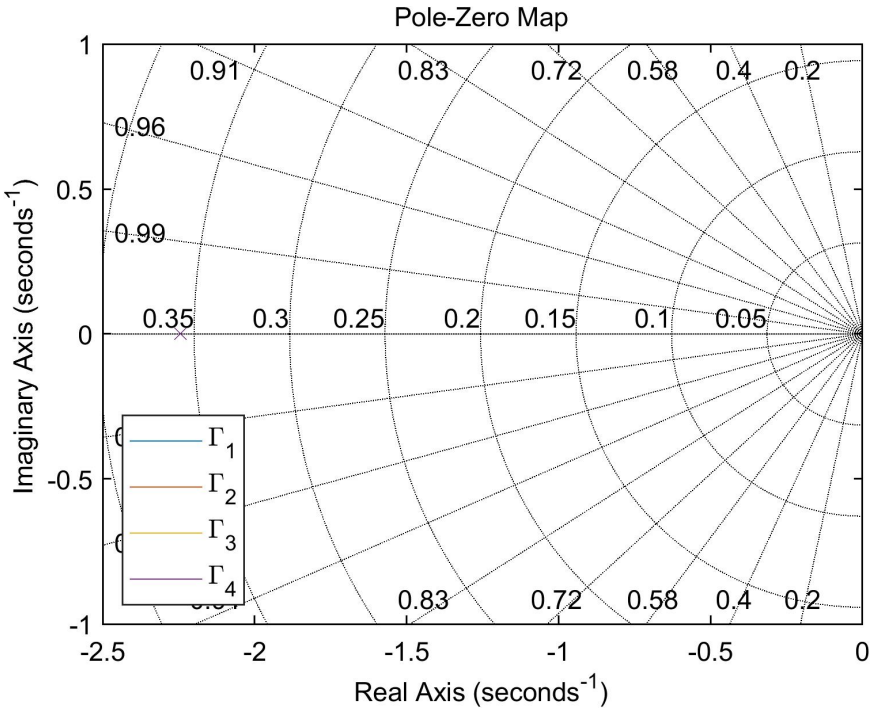


Figure 4.9: Case 3

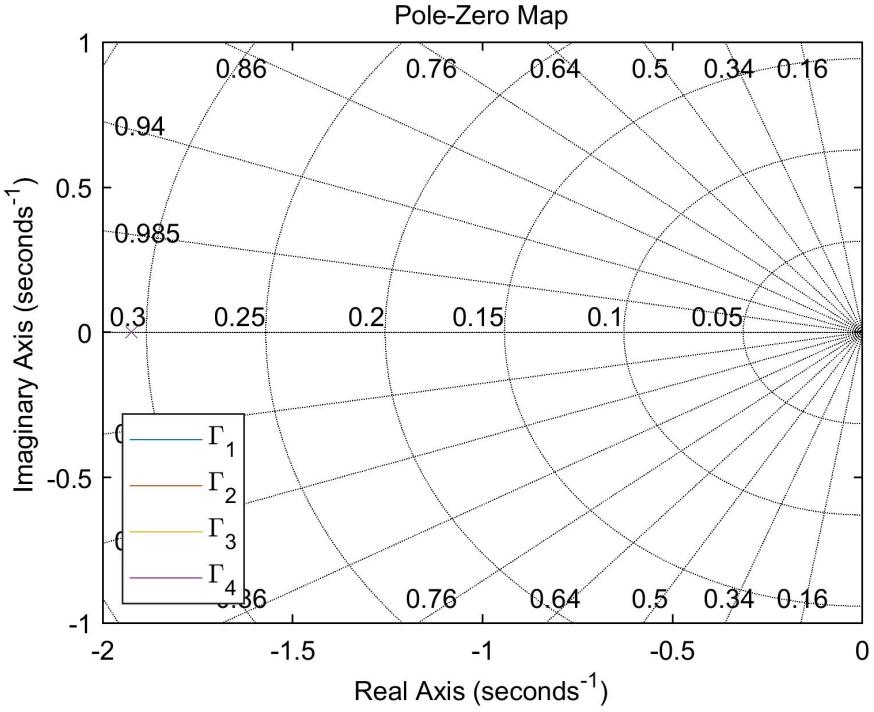


Figure 4.10: Case 4

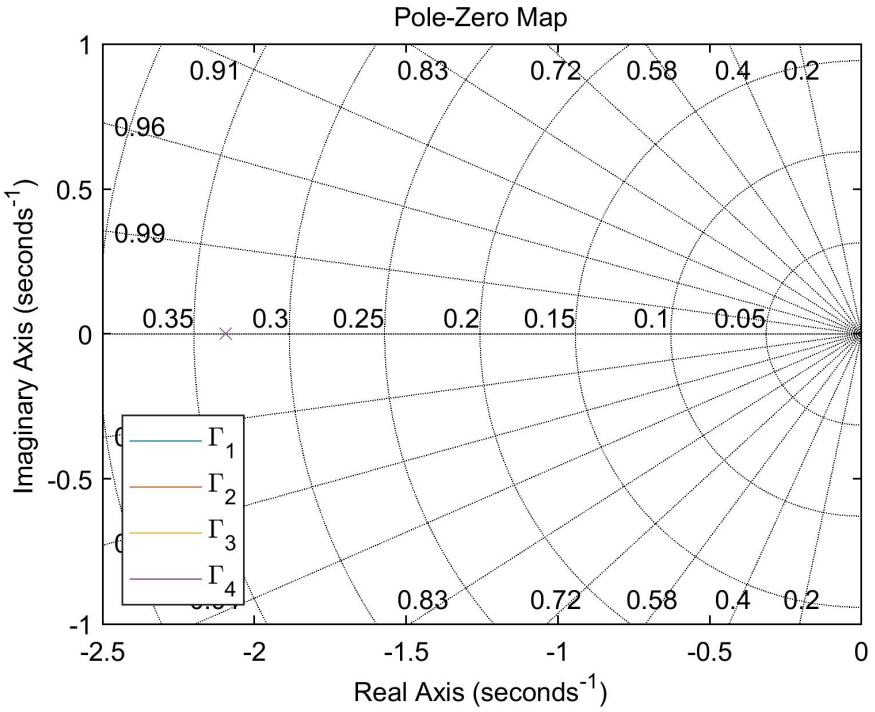


Figure 4.11: Case 5

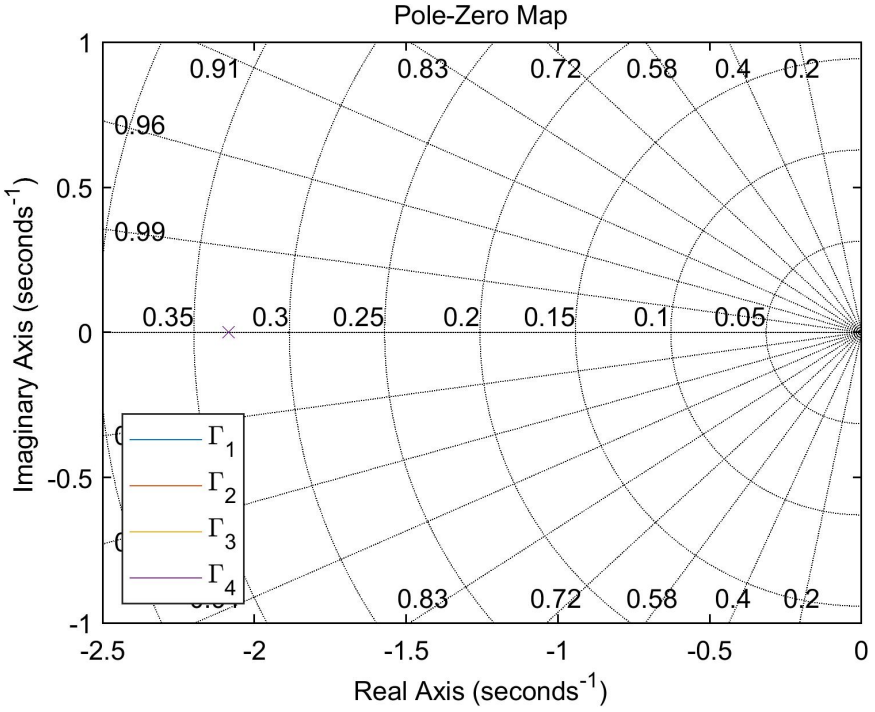


Figure 4.12: Case 6

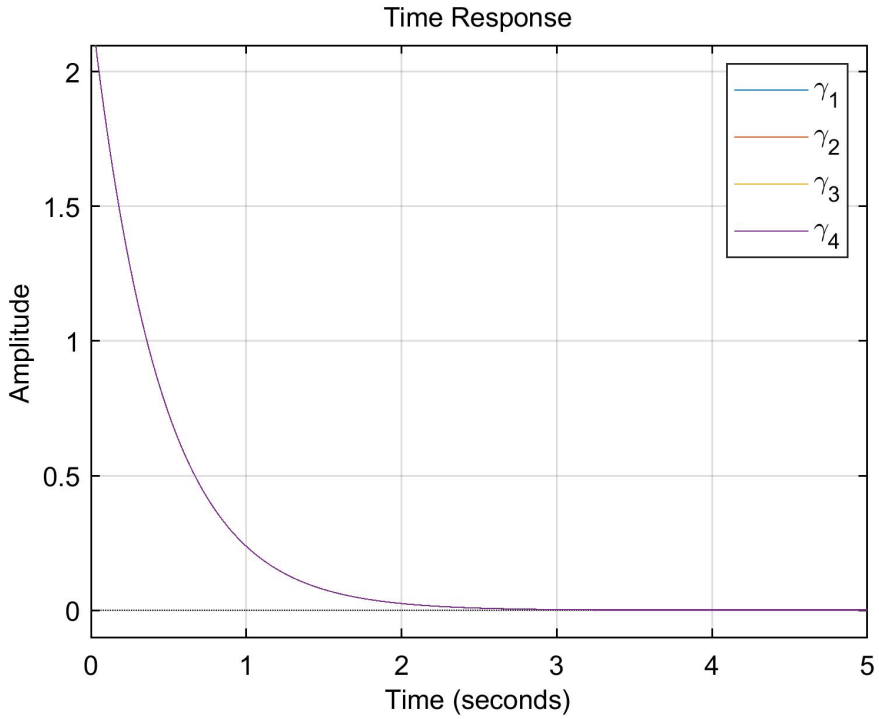


Figure 4.13: IR functions of homogeneous string with $\tau_i = 0.16$ for case 3

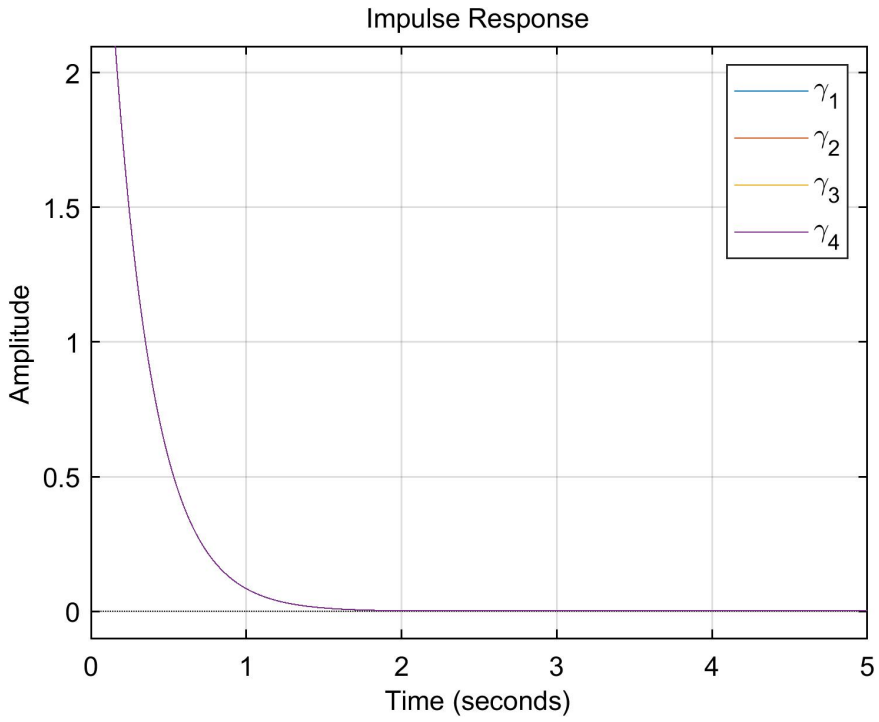


Figure 4.14: IR functions of homogeneous string with $\tau_i = 0.64$ for case 6

Secondly, heterogeneous strings are to be considered. From here onwards, in this section, to build on top of the discussion held above, we will concentrate on sharing the results for cases 3 and 6. We start heterogeneous examples off with the simulations of two different strings, whose parameter values are as given in Tables 4.2 and 4.3. The driveline dynamics constants of the first are close to the lower bound of acknowledged values in literature (Equation (4.2)), and the latter have them near the upper bound. The resultant pole-zero maps, bode plots and impulse response functions for both simulations with the controllers optimized in cases 3 and 6 are given in Figures 4.15 to 4.17 and 4.21 to 4.23. Also, the corresponding acceleration, velocity and position signals are given in Figures 4.18 to 4.20 and 4.24 to 4.26. Referring to Equation (2.10), it is evident from bode plots that all synthesized controllers yield $L_2$ string stability. Comparing the infinity norm of accelerations also clearly indicates strict $L_\infty$ string stability. With these two results the optimization based controller synthesis method proves itself to be useful for the range of driveline dynamics constant values which are deemed as realistic ones.

| $i$ | $\theta_i$ | $\phi_i$ | $\tau_i$ |
|---|---|---|---|
| 0 | 0 | 0 | 0.14 |
| 1 | 0 | 0 | 0.16 |
| 2 | 0 | 0 | 0.18 |
| 3 | 0 | 0 | 0.22 |
| 4 | 0 | 0 | 0.24 |

Table 4.2: Zero delay heterogeneous string parameter set 1

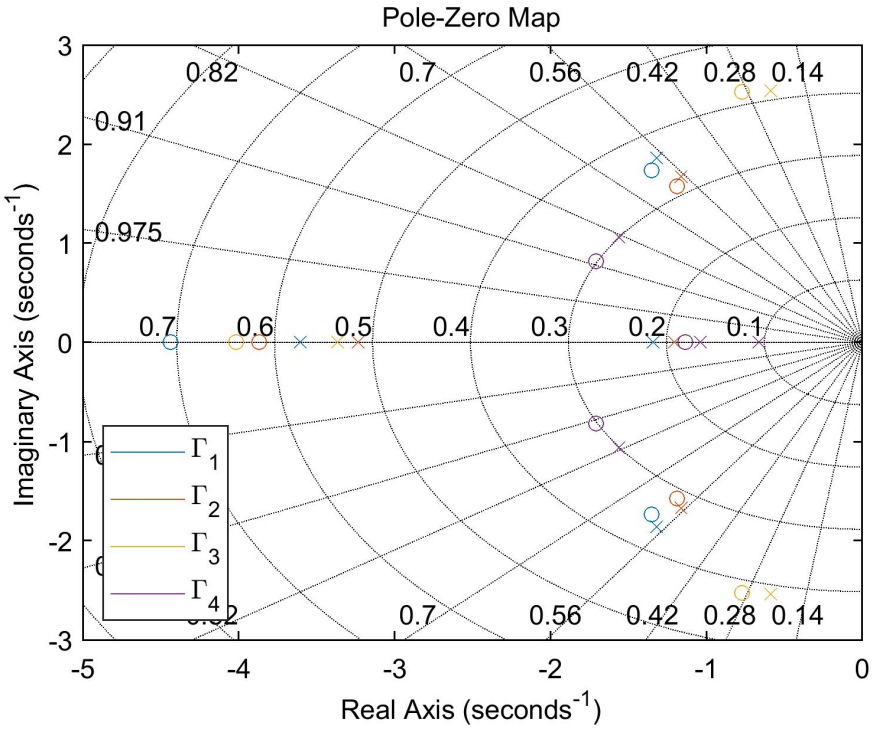


Figure 4.15: Pole-zero maps of heterogeneous string in Table 4.2 for case 3

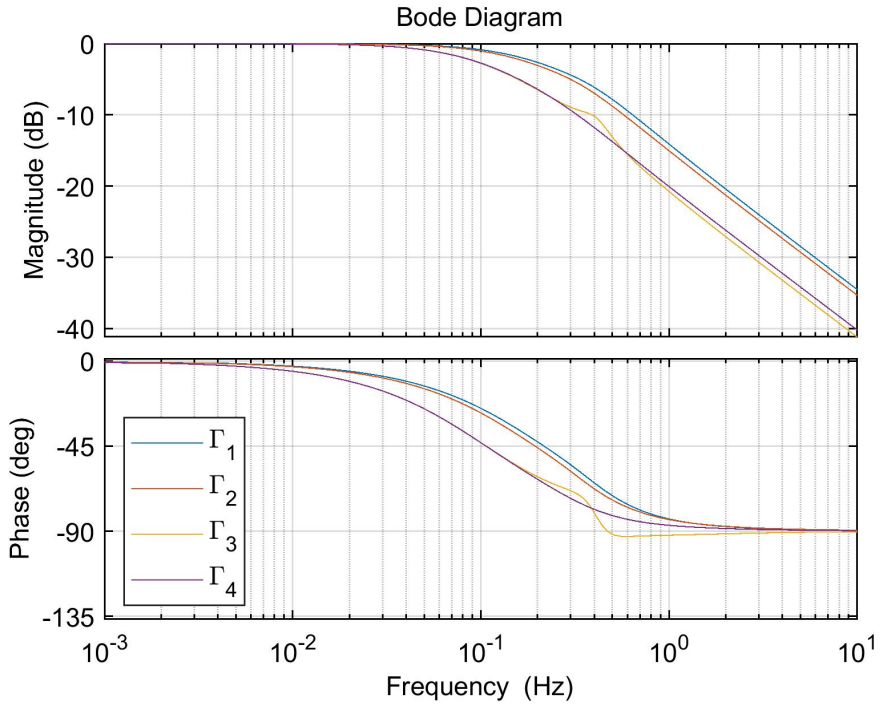


Figure 4.16: Corresponding Bode plots

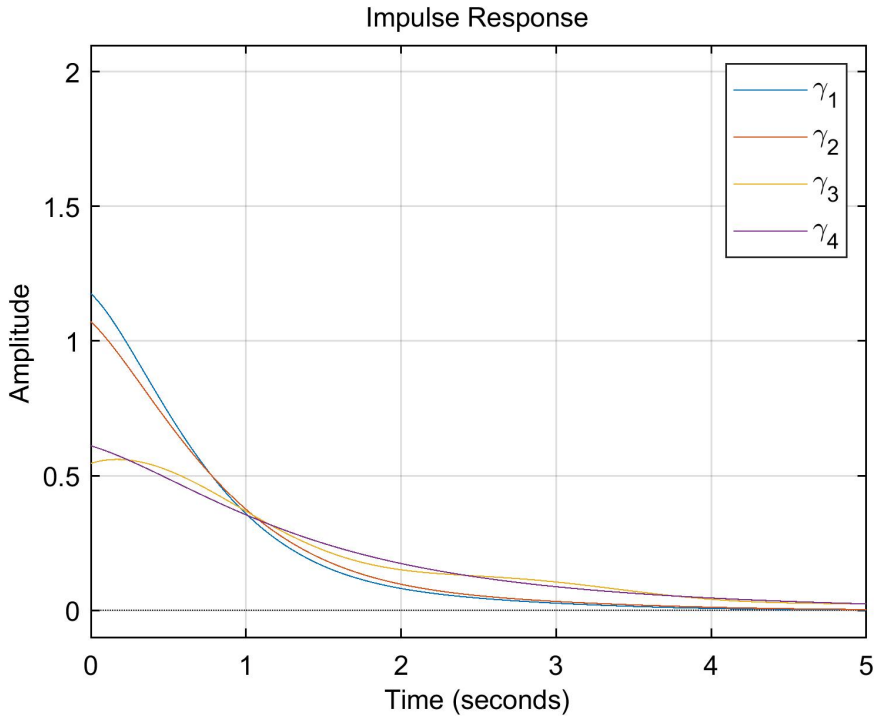


Figure 4.17: Corresponding impulse responses

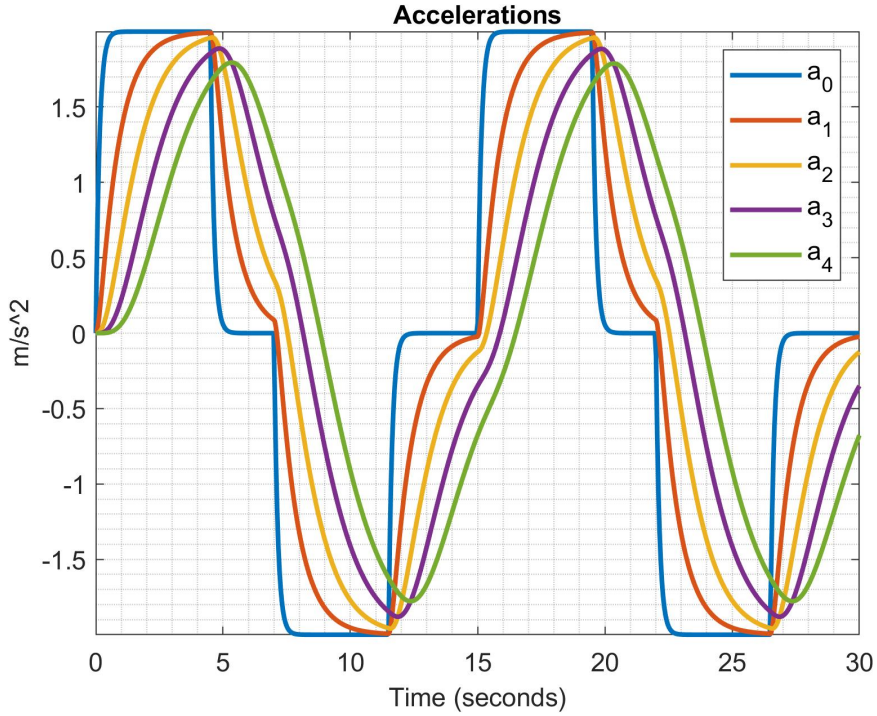


Figure 4.18: Resulting accelerations in response to input in Figure 4.5

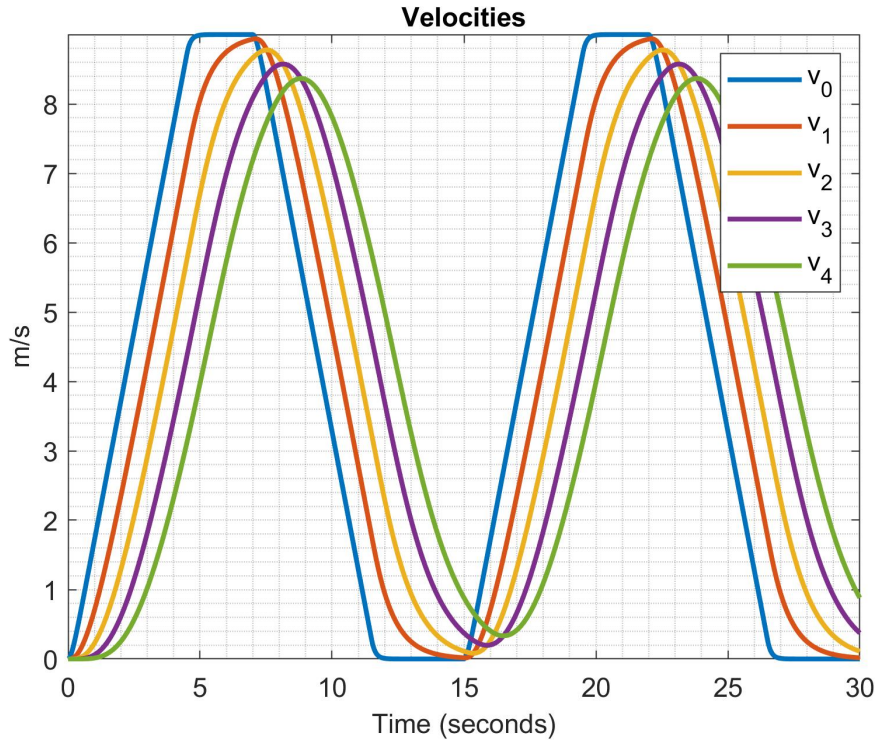


Figure 4.19: Corresponding velocities

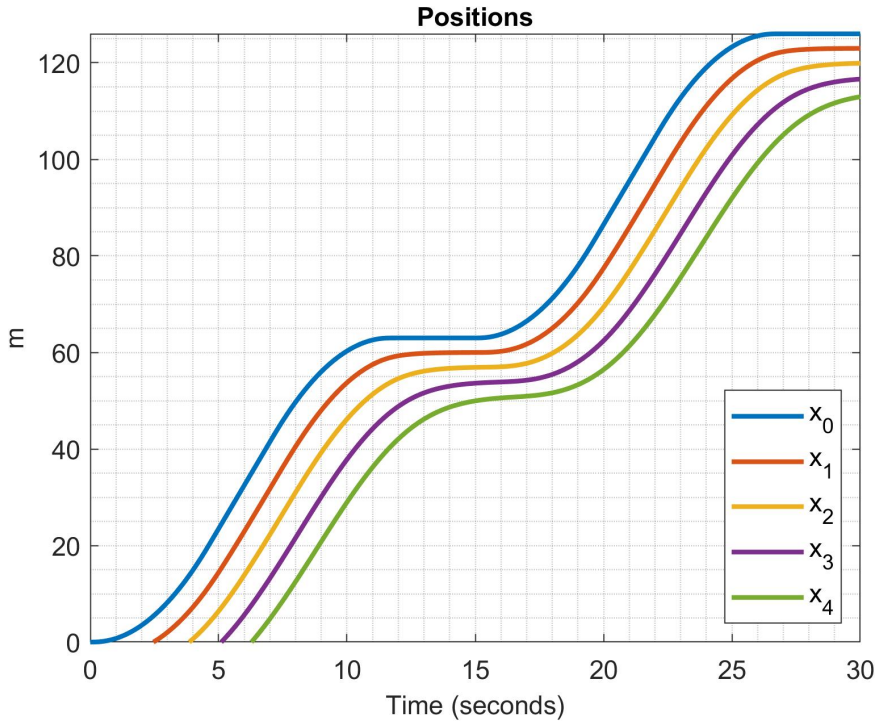


Figure 4.20: Corresponding positions

| $i$ | $\theta_i$ | $\phi_i$ | $\tau_i$ |
|---|---|---|---|
| 0 | 0 | 0 | 0.70 |
| 1 | 0 | 0 | 0.72 |
| 2 | 0 | 0 | 0.74 |
| 3 | 0 | 0 | 0.76 |
| 4 | 0 | 0 | 0.78 |

Table 4.3: Zero delay heterogeneous string parameter set 2

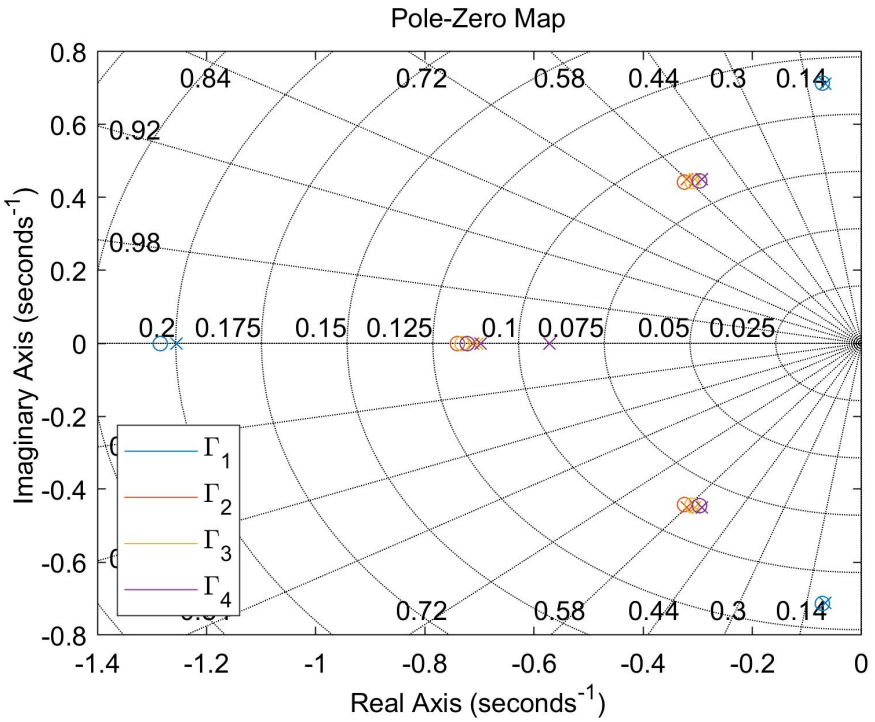


Figure 4.21: Pole-zero maps of heterogeneous string in Table 4.3 for case 6

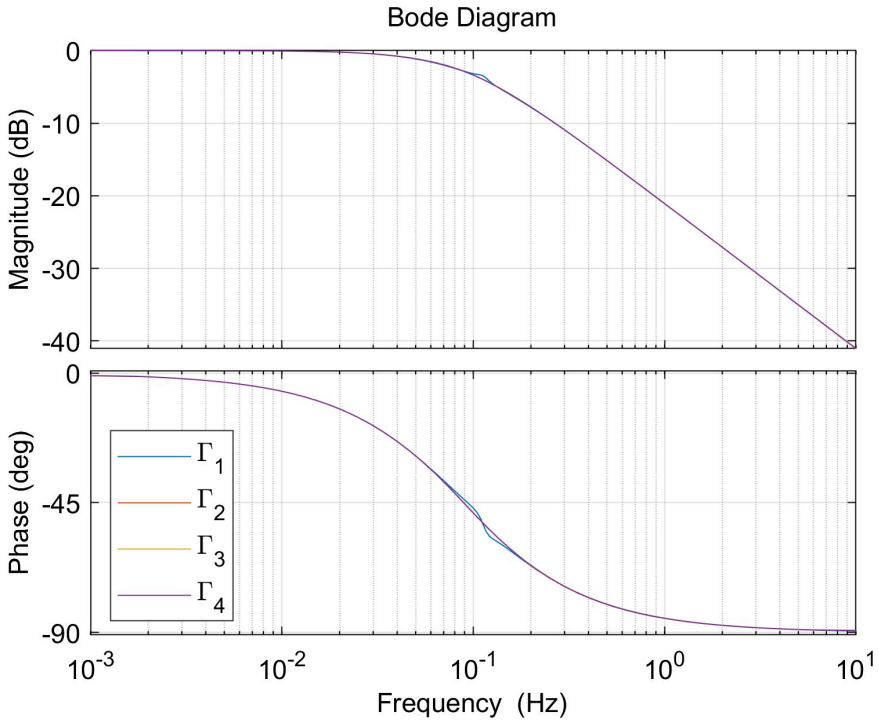


Figure 4.22: Corresponding Bode plots

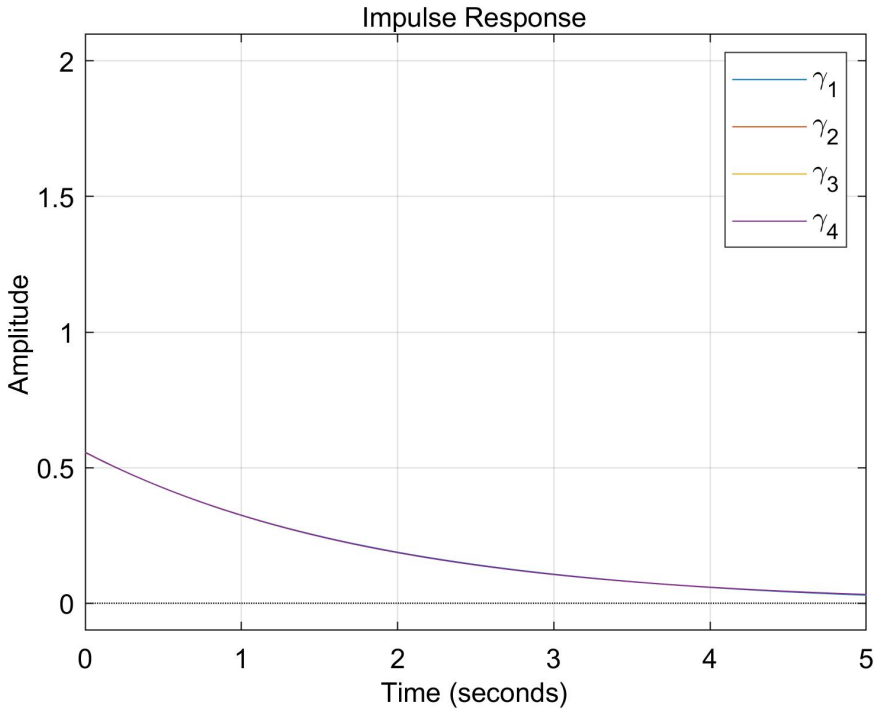


Figure 4.23: Corresponding impulse responses

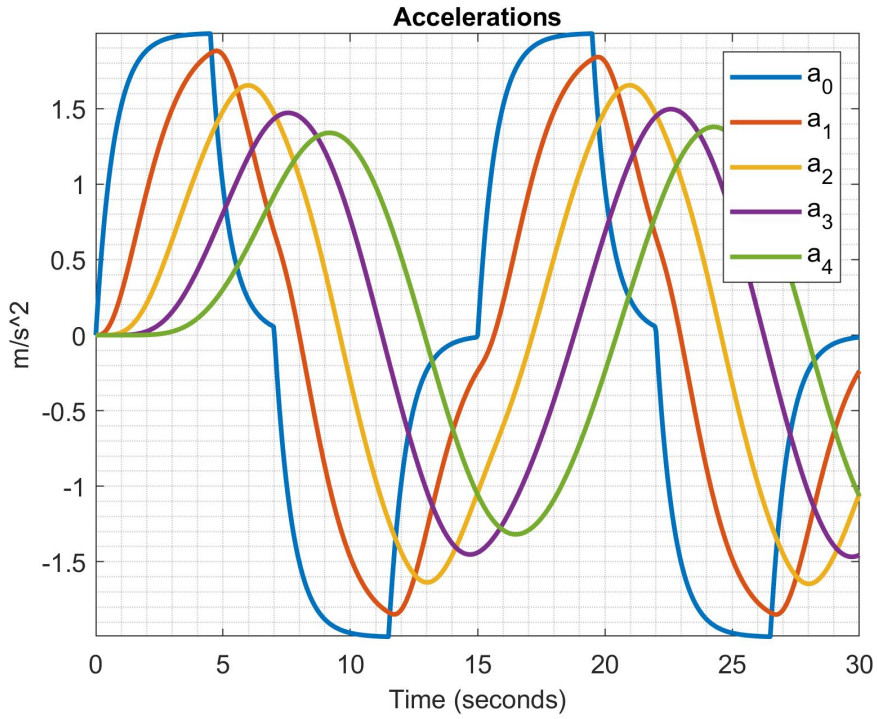


Figure 4.24: Resulting accelerations in response to input in Figure 4.5

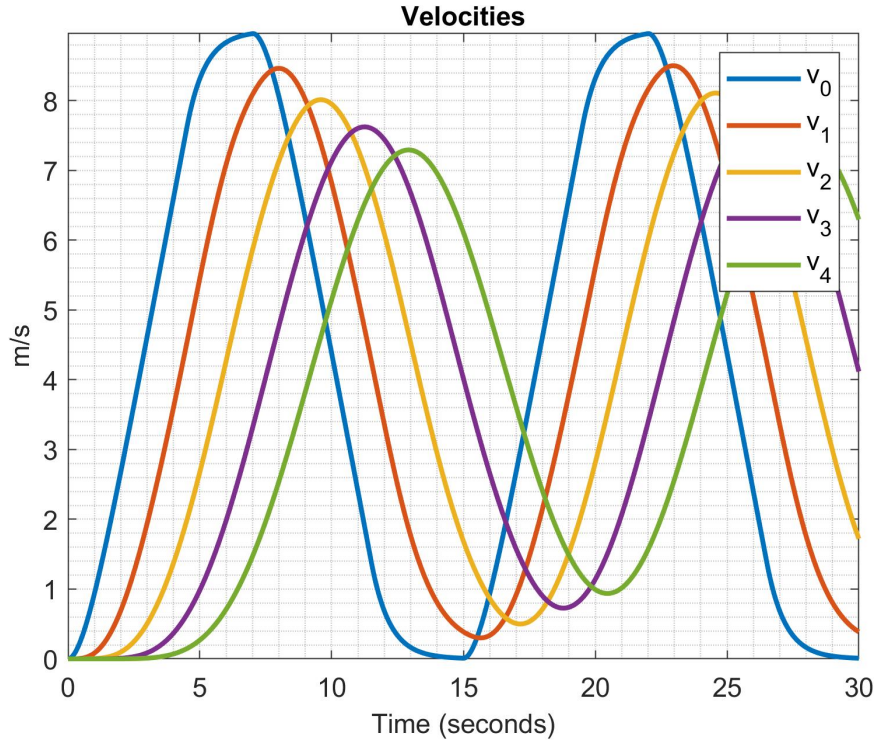


Figure 4.25: Corresponding velocities

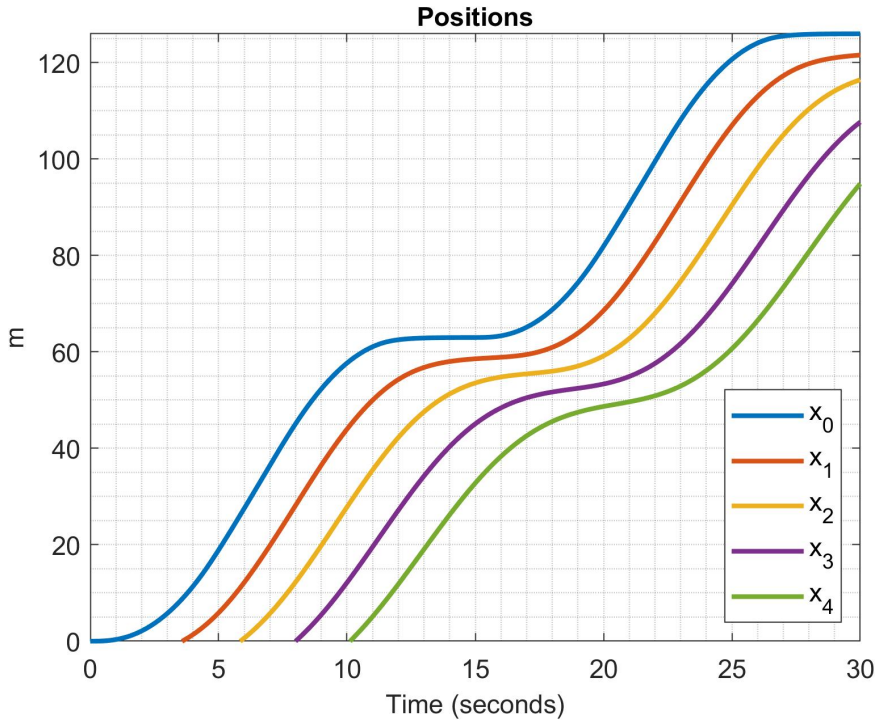


Figure 4.26: Corresponding positions

At this point, it is essential to revisit the definition of the optimization problem laid out in section 3.3. Before proceeding into investigation of effects of delays, certain constraints that were imposed to yield positive impulse response transfer functions are needed to be checked and analyzed. To recall, there are fundamentally two constraints needed to be checked which are given in Equations (3.15) and (3.26). It has been recorded that, in none of the heterogeneous strings these two constraints were achieved. In fact, when the former of the two constraints is violated, the expression for Equation (3.25) becomes invalid since the imaginary pole pairs will start introducing different time domain expressions into the impulse response functions, whose generic form are given as

$$e^{at}sin(bt). \tag{4.3}$$

However, reiterating that the whole process was designed to force the optimizer to push the resulting transfer function to attain positive impulse response by trying to fulfill the sufficient conditions which are more than necessary ones, this does not necessarily mean that strict $L_\infty$ string stability with positive impulse response transfer functions is unachievable. Actually, examining the coefficients of time domain terms

would shed light on the ambiguity of how come the optimization process manages to return positive impulse responses. Though, assuming complex conjugate pair of poles in Equation (3.14) and generalizing Laguerre's [24] proposition to complex decay factors would be beyond the scope of this thesis work. Still, taking the outputs generated by the optimizer into account, there can be comments made on answering this question. The most reasonable way to interpret the positive impulse responses observed throughout the experiments with a variety set of parameters is to think that the exponential terms in time domain expressions of complex poles, Equation (4.3), are decaying so fast such that the sinusoids become unable to distort the impulse response function causing negativity.

| $i$ | $\theta_i$ | $\phi_i$ | $\tau_i$ |
|---|---|---|---|
| 0 | 0 | 0 | 0.16 |
| 1 | 0 | 0 | 0.32 |
| 2 | 0 | 0 | 0.48 |
| 3 | 0 | 0 | 0.64 |
| 4 | 0 | 0 | 0.72 |

Table 4.4: Zero delay heterogeneous string parameter set 3

Finally, we would like to draw attention to a specific case of heterogeneous strings. It is the case where within a string, subsequent vehicles' driveline dynamics differ dramatically. In other words, the parameter sets where a predecessor-follower pair has huge difference in terms of their driveline dynamics. One such exemplary parameter set is given in Table 4.4. In such simulations, it was observed that some of the controllers may yield unstable impulse responses regardless of the case of optimization process being run. This might be causing certain constraints and the objective function to be pushed in such ways that the solver cannot converge to any feasible solution where it satisfies string stability. It might even be the case that attaining string stability with positive impulse transfer functions becomes impossible in such scenarios. This phenomena occurring with the choice of range of driveline dynamics constant, intuitively tells us that it can generate controllers for strings which are composed of alike vehicles i.e. cars with cars and trucks with trucks. In short, it must

be stated that when the driveline dynamics parameters are far apart from each other for some predecessor-follower vehicle pairs, the developed optimization based controller tuning is not working properly. Enlightening the reason behind this requires further investigation of constraints and defined objective function of the optimization problem.

## 4.3 Communication Delay

In order to see the delays effects purely, we will also fix the headway time constant which was an optimization parameter *as defined earlier* by equating its upper and lower bounds to make it a constant value. Throughout this section,

$$h_i = 1 \ , \ i = 1, 2, 3, 4 \tag{4.4}$$

will be the utilized headway time gap. Also, as one of the two delay parameters being examined, the other will be left loose to let the delay of concern manifest its effect more clearly.

Firstly, we are going to sweep the communication delay $\theta_i$ with the parameter set in Table 4.5 for the evaluation of the effect of communication delays. Secondly, simulations with the fixed values in Table 4.6 will be shared for observing the actuator delay effect by sweeping $\phi_i$. In short, it can be said that we are going to sweep the two types of delays one by one up to their limits.

One last thing to note for having intuition over these simulations is that the chosen $\tau_i$ values in Tables 4.5 and 4.6 somewhat represent a string like the one in Figure 2.2, i.e. starting with a smaller driveline dynamics constant or equivalently a more agile vehicle and being followed by a more sluggish one.

We swept the communication delay with the values in Equations (4.5) to (4.8)

$$1^{st}Run : \theta_i = 0.025s \tag{4.5}$$

$$2^{nd}Run : \theta_i = 0.125s \tag{4.6}$$

$$3^{rd}Run : \theta_i = 0.250s \tag{4.7}$$

$$4^{th}Run : \theta_i = 0.500s \tag{4.8}$$

| $i$ | $h_i$ | $\phi_i$ | $\tau_i$ |
|---|---|---|---|
| 0 | 1 | 0.02 | 0.100 |
| 1 | 1 | 0.02 | 0.125 |
| 2 | 1 | 0.02 | 0.150 |
| 3 | 1 | 0.02 | 0.175 |
| 4 | 1 | 0.02 | 0.200 |

Table 4.5: Fixed parameter set to test communication delay tolerance

The effect of communication delay was examined by increasing $\theta_i$ gradually. In Figures 4.27 to 4.32, the resultant impulse responses of the optimized controllers are given for different cases mentioned in optimization problem formulation. In the solution of optimization problem, the cost function was formed so that the closest pole to the imaginary axis can be pushed as far as possible.

From Figures 4.27 to 4.32, it is seen that not in all cases of the optimization problem a positive impulse response CACC controllers are achievable, for instance, in cases 2 and 4 the zero line was slightly crossed. Note that there might be achievable positive impulse response controllers within the regions defined by those two cases, however, it is certain that with the approach we adopted it was not possible to converge to positive impulse response controllers in cases 2 and 4. On the other hand, for the rest of the cases, it successfully converged to positive impulse response controllers.

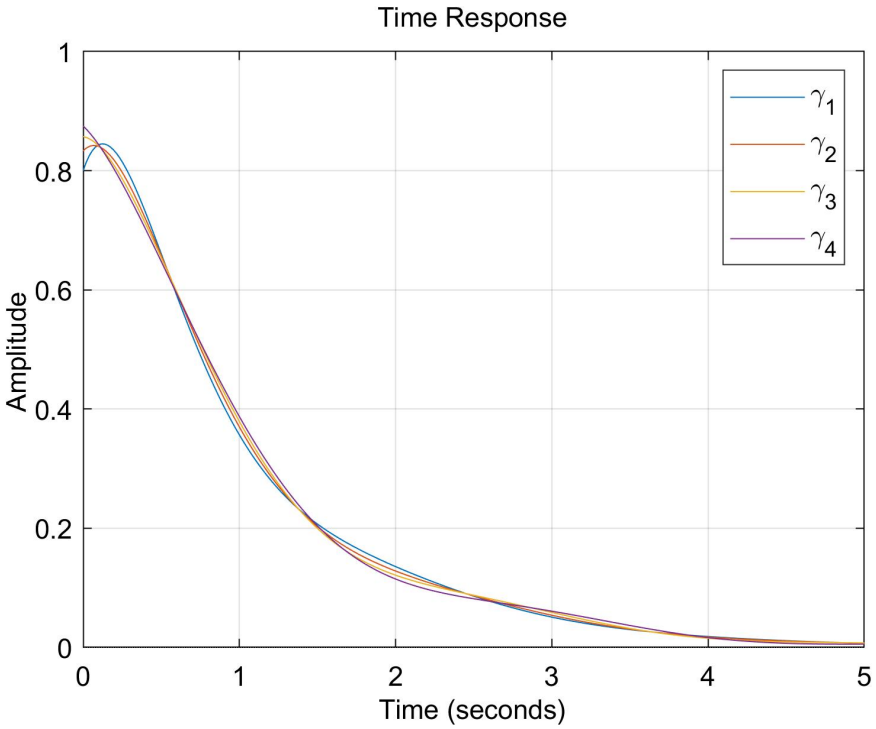


Figure 4.27: Impulse response for the resultant controller in case 1

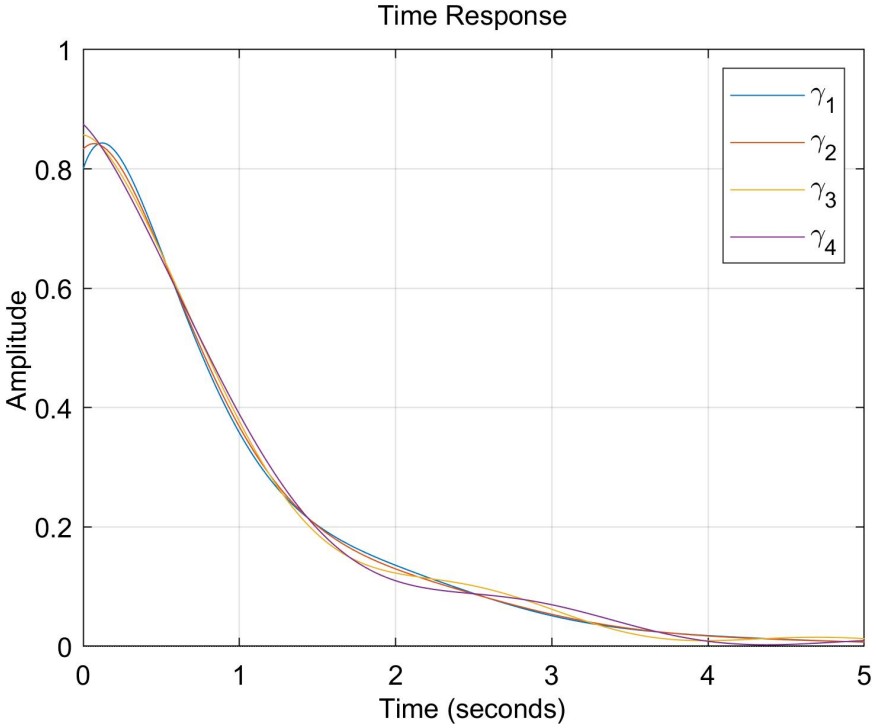


Figure 4.28: Impulse response for the resultant controller in case 2

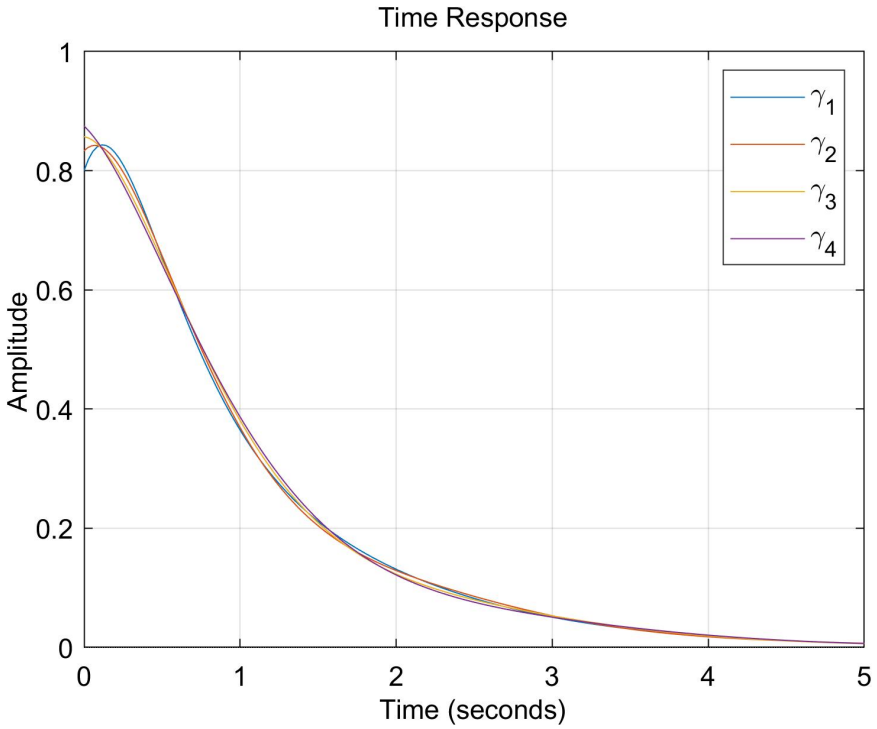


Figure 4.29: Impulse response for the resultant controller in case 3

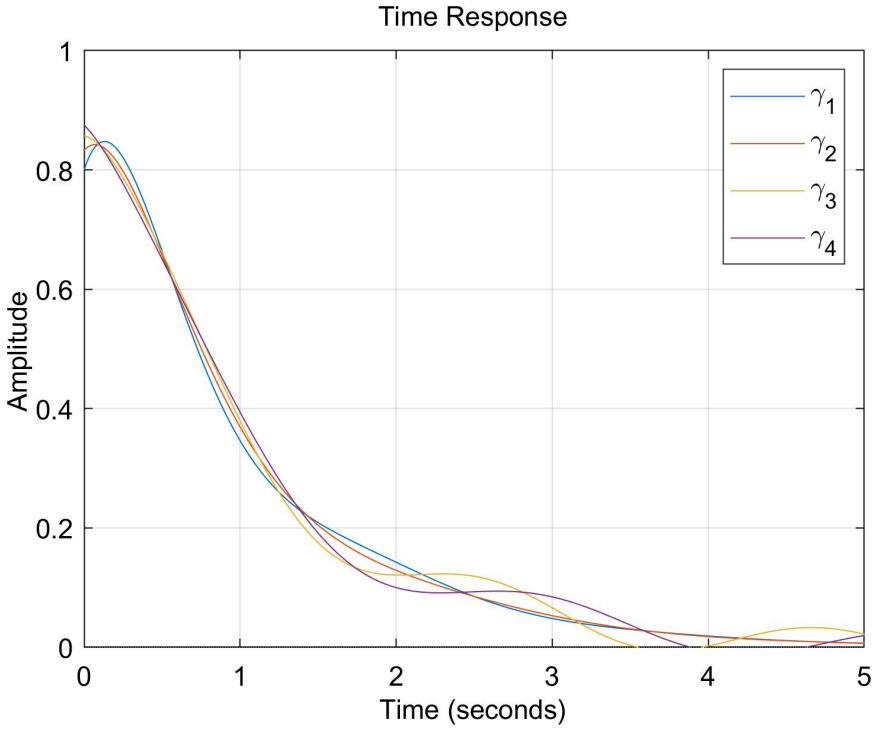


Figure 4.30: Impulse response for the resultant controller in case 4

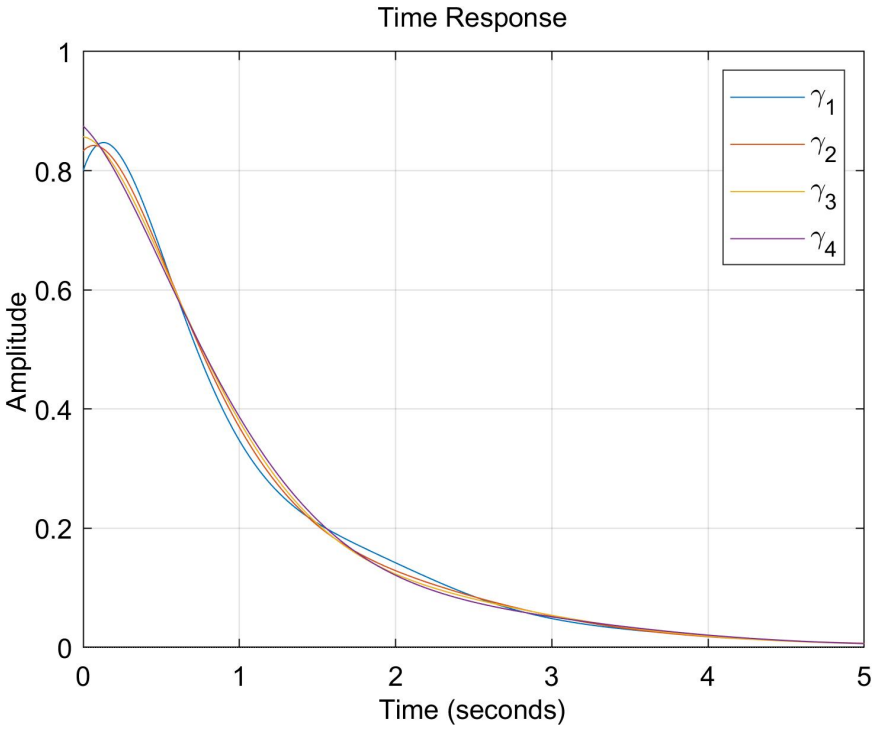


Figure 4.31: Impulse response for the resultant controller in case 5

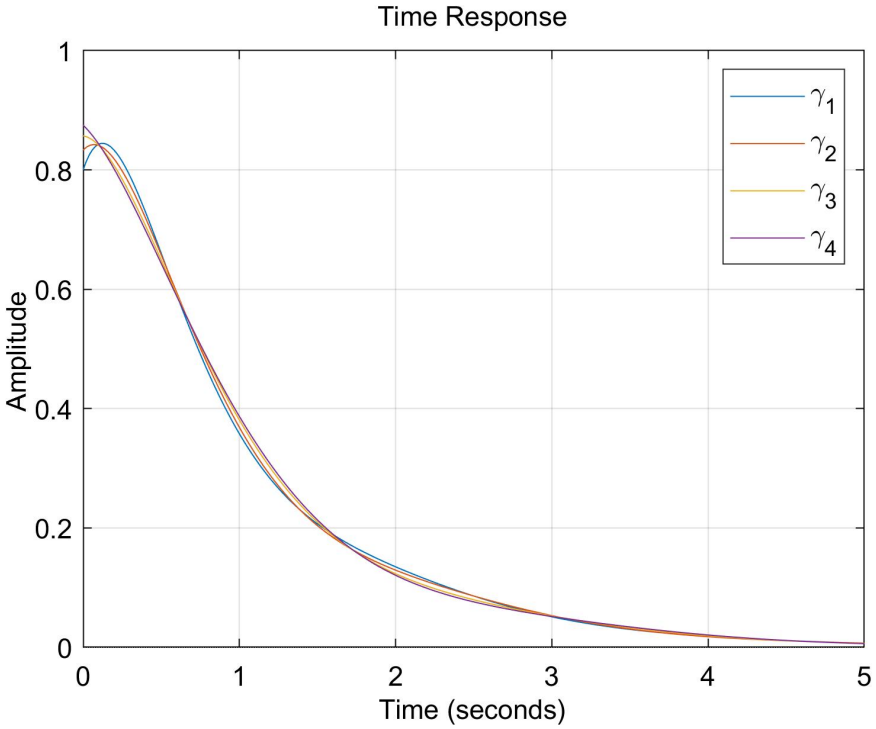


Figure 4.32: Impulse response for the resultant controller in case 6

Nonetheless, the acceleration signals for each case show $L_2$ and $L_\infty$ string-stable behavior as can be seen in Figures 4.33 to 4.38. These are the acceleration response to the third type of input signal given in Figure 4.6 simulated with $25ms$ communication delays between all vehicles. The responses are so close to each other such that they cannot be distinguished unless zoomed in. There is no difference other than very little changes in the speed of the transient responses of the vehicles to step inputs.

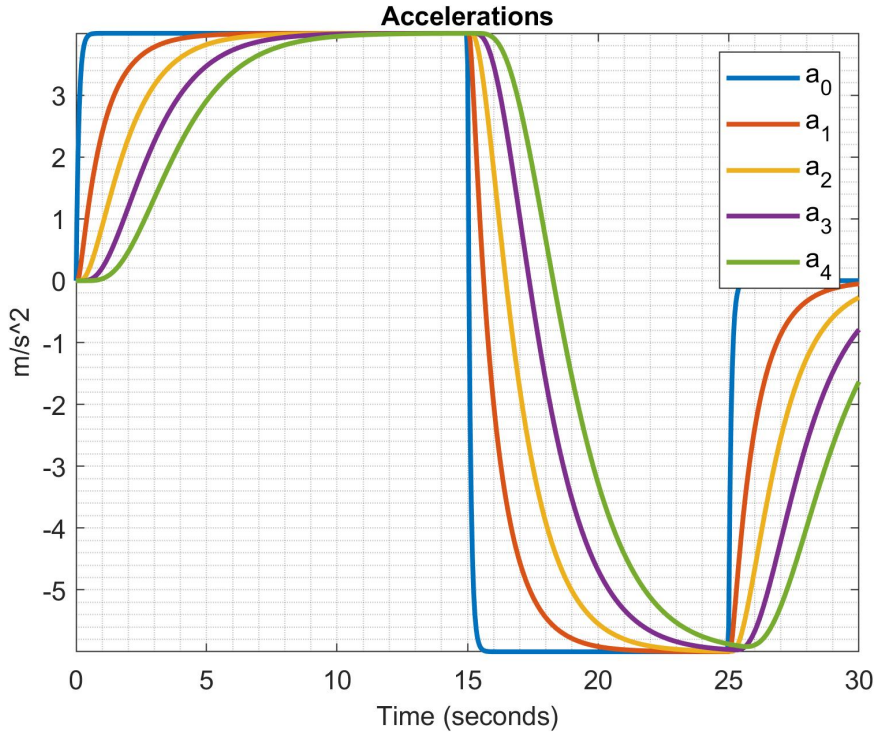


Figure 4.33: Accelerations for the synthesized controllers in case 1 for $\theta_i = 25ms$

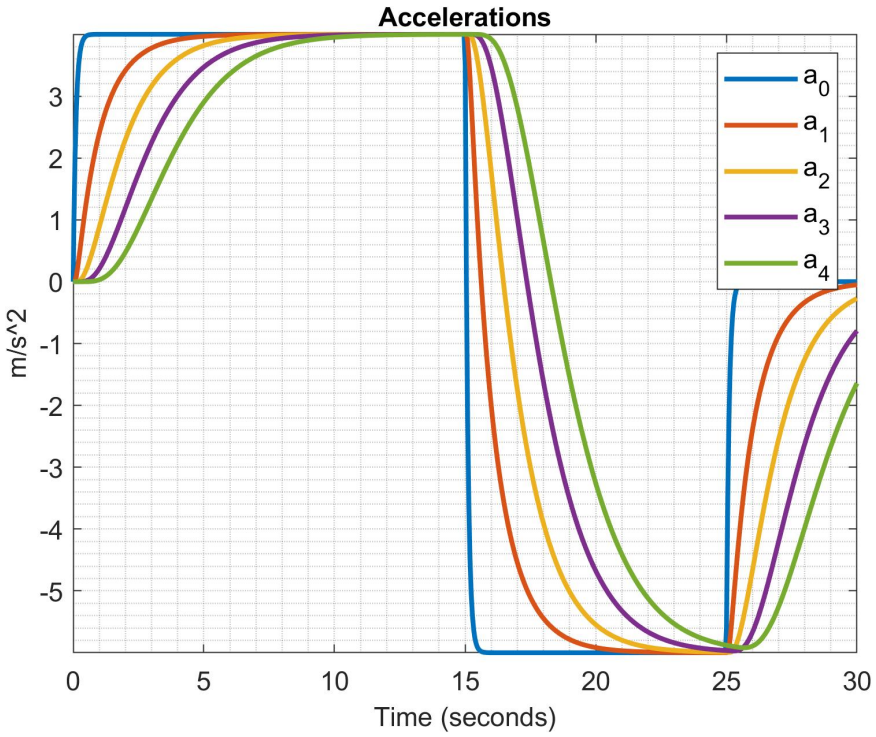


Figure 4.34: Accelerations for the synthesized controllers in case 2 for $\theta_i = 25ms$

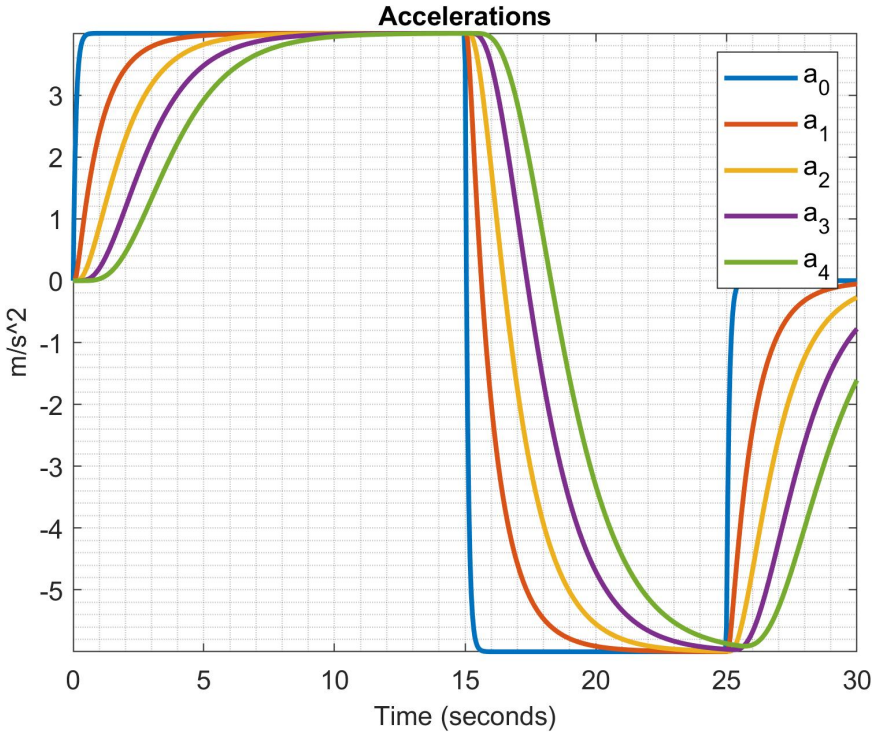


Figure 4.35: Accelerations for the synthesized controllers in case 3 for $\theta_i = 25ms$

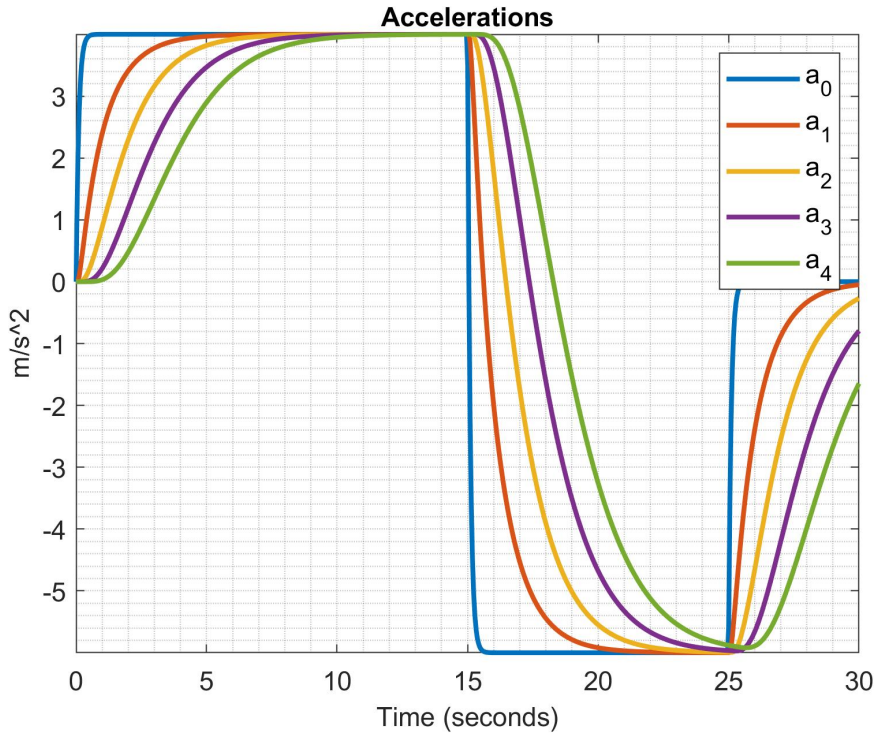


Figure 4.36: Accelerations for the synthesized controllers in case 4 for $\theta_i = 25ms$

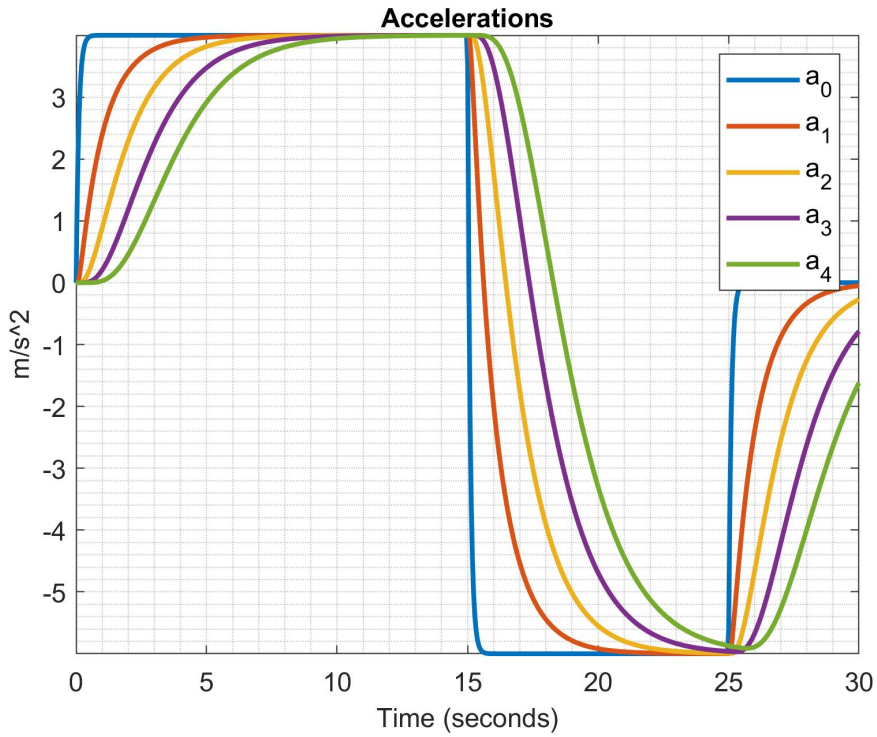


Figure 4.37: Accelerations for the synthesized controllers in case 5 for $\theta_i = 25ms$

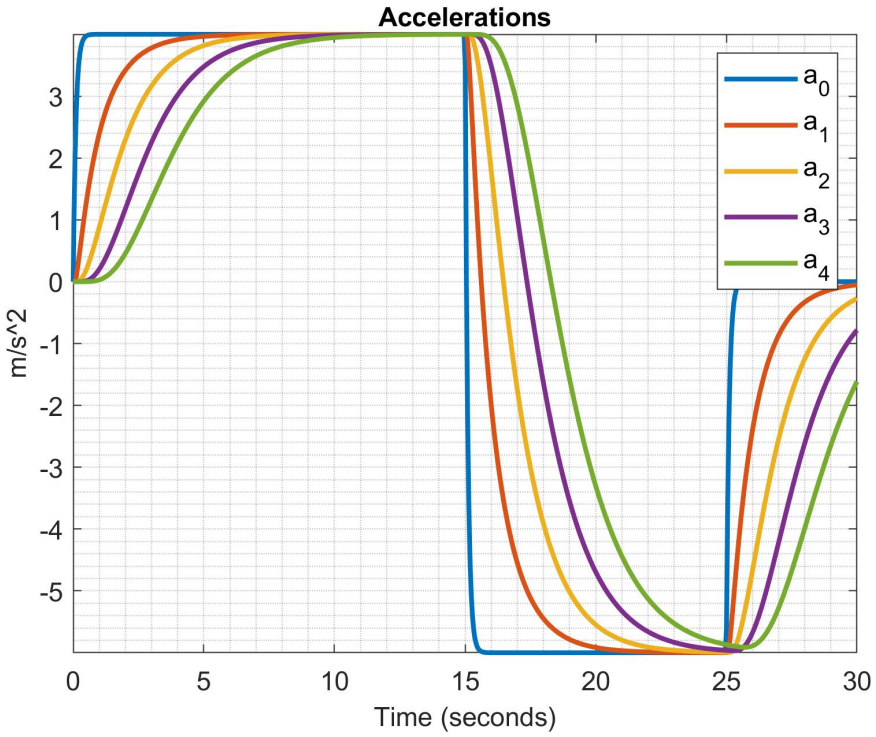


Figure 4.38: Accelerations for the synthesized controllers in case 6 for $\theta_i = 25ms$

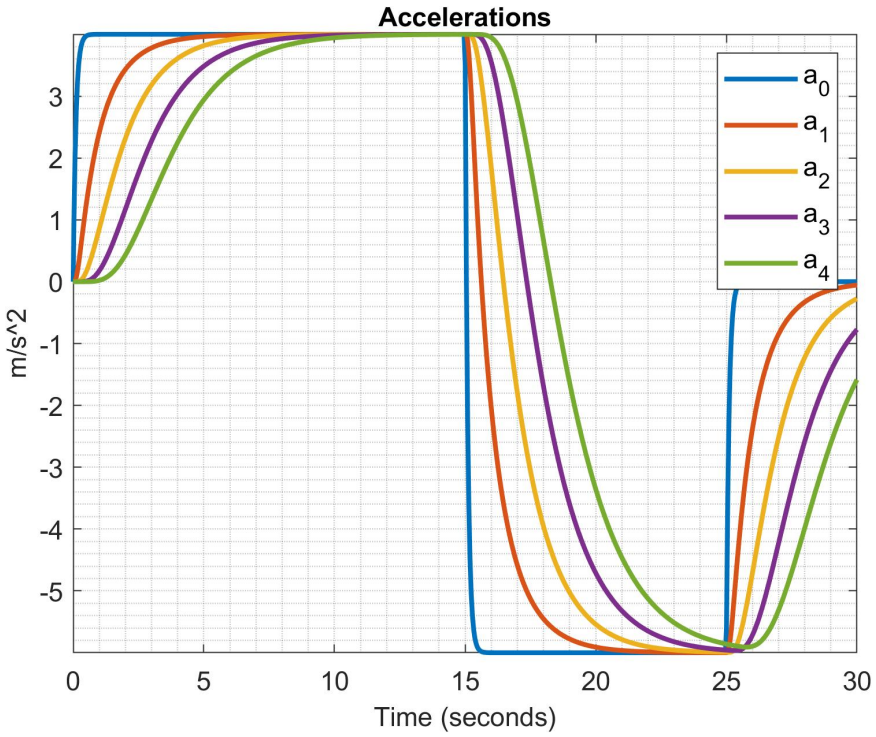


Figure 4.39: Case 6, Communication delay increased to $\theta_i = 125ms$

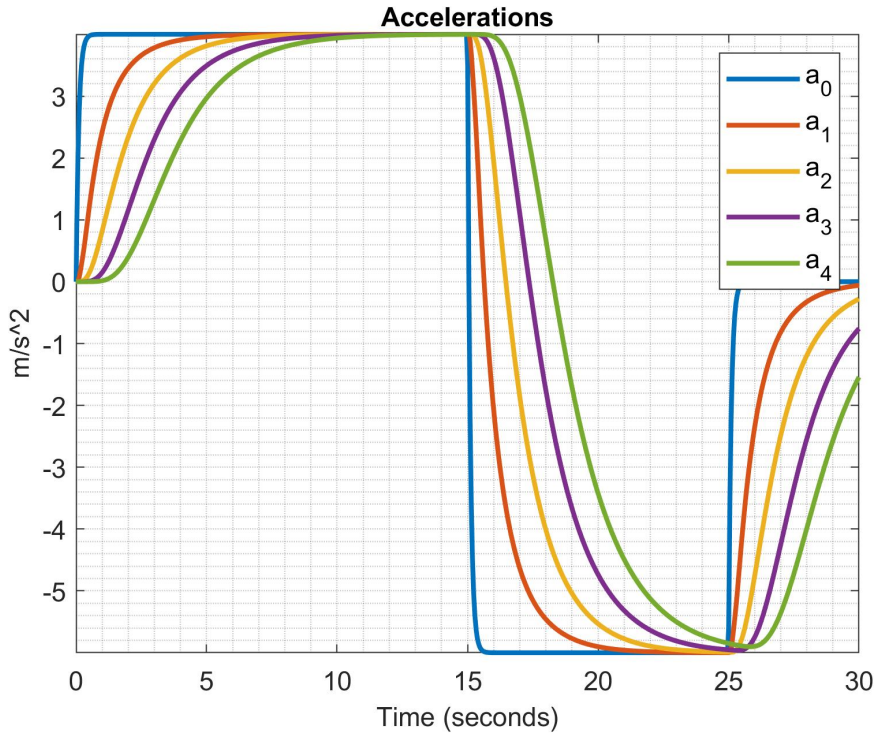


Figure 4.40: Case 6, Communication delay increased to $\theta_i = 250ms$

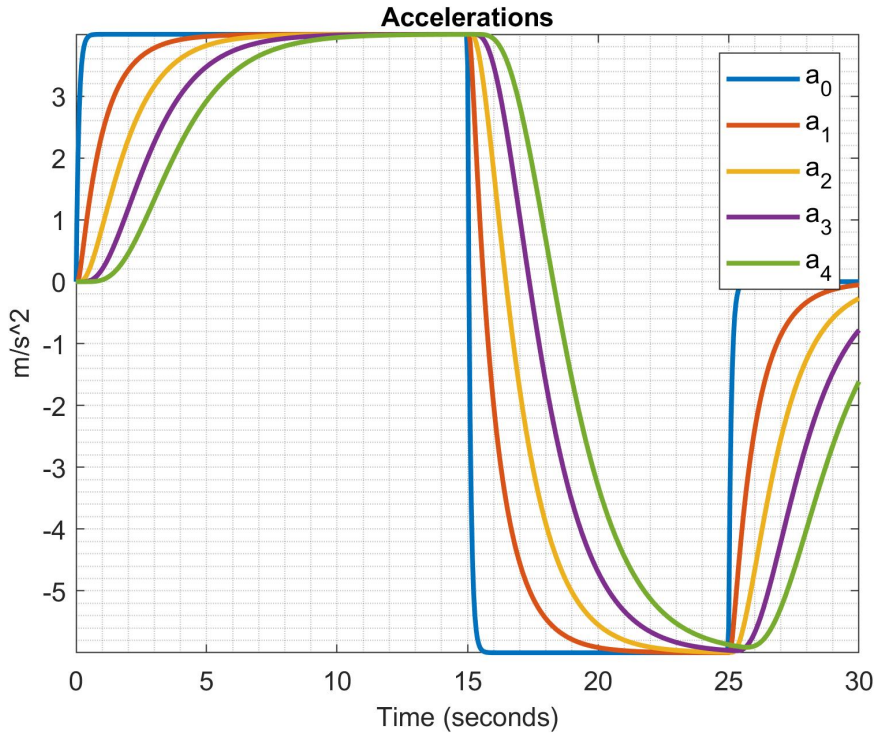


Figure 4.41: Case 6, Communication delay increased to $\theta_i = 500ms$

For example, in Figure 4.42, since the condition in Equation (2.10) is fulfilled, $L_2$ string stability is attained.

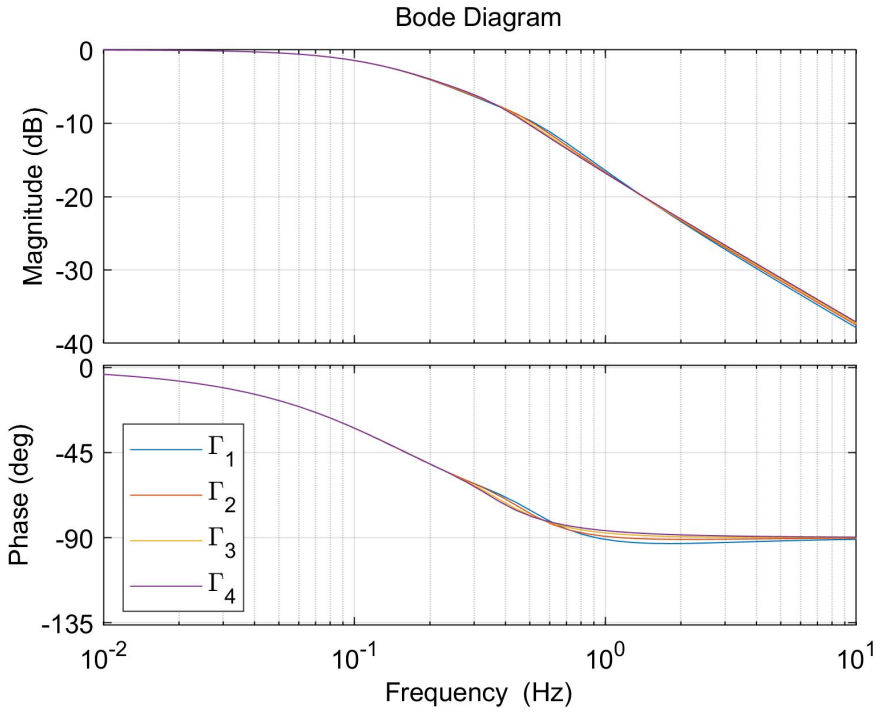


Figure 4.42: Bode plots for the resultant controllers in case 6

The swept values of $\theta_i$ in Equations (4.5) to (4.8) resulted in the following acceleration signals, having not much significant changes except for the slower transient response effect, which are given in Figures 4.38 to 4.41.

## 4.4 Actuator Delay

For understanding the significance of actuator delay, which directly translates into how late an action is taken by the feedback controller, it has been swept through the values given in Equations (4.9) to (4.11) while having the rest of the parameters fixed at the values given in Table 4.6. It is evident from Figures 4.43 to 4.46 that the actuator delay is a much more sensitive parameter than communication delay, in that, in any case of optimal controller solutions, approximately more than 60 milliseconds cannot be tolerated.

Considering that the given values in Equation (4.2) ranges up to 200 milliseconds, there needs to be an improvement made. If the optimization problem cannot be enhanced to yield such improvement, there has to be a trade off taking place which is what we are going to point at in the set of simulations started by values in Table 4.7.

| $i$ | $h_i$ | $\theta_i$ | $\tau_i$ |
|---|---|---|---|
| 0 | 1 | 0.02 | 0.100 |
| 1 | 1 | 0.02 | 0.125 |
| 2 | 1 | 0.02 | 0.150 |
| 3 | 1 | 0.02 | 0.175 |
| 4 | 1 | 0.02 | 0.200 |

Table 4.6: Fixed parameter set to test actuator delay tolerance

$$1^{st}Run : \phi_i = 0.025s \tag{4.9}$$

$$2^{nd}Run : \phi_i = 0.050s \tag{4.10}$$

$$3^{rd}Run : \phi_i = 0.065s \tag{4.11}$$

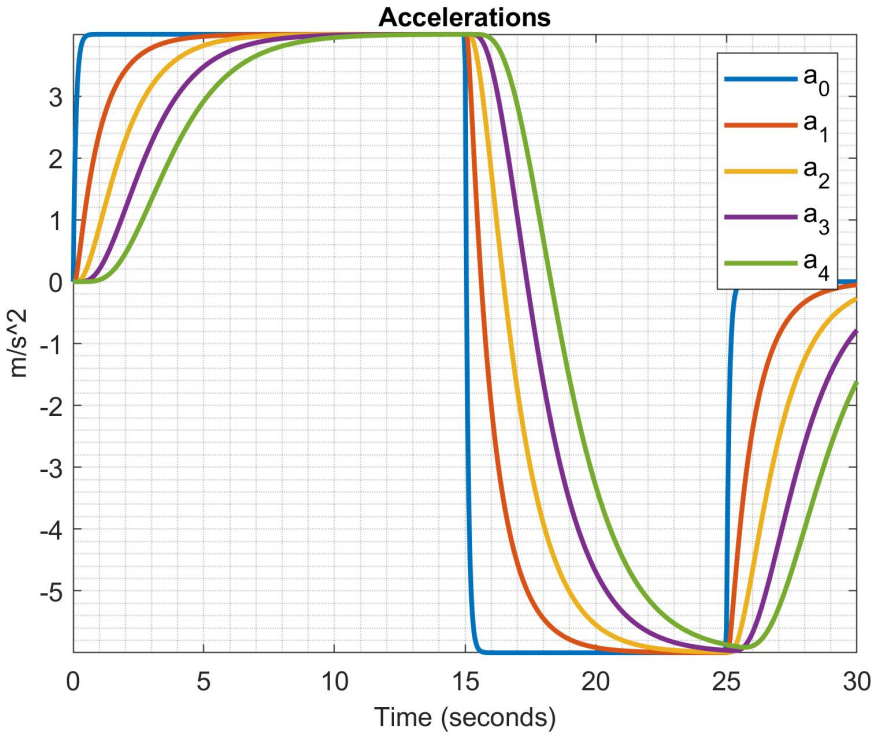


Figure 4.43: Accelerations for the controller in case 6 for 25ms actuator delay

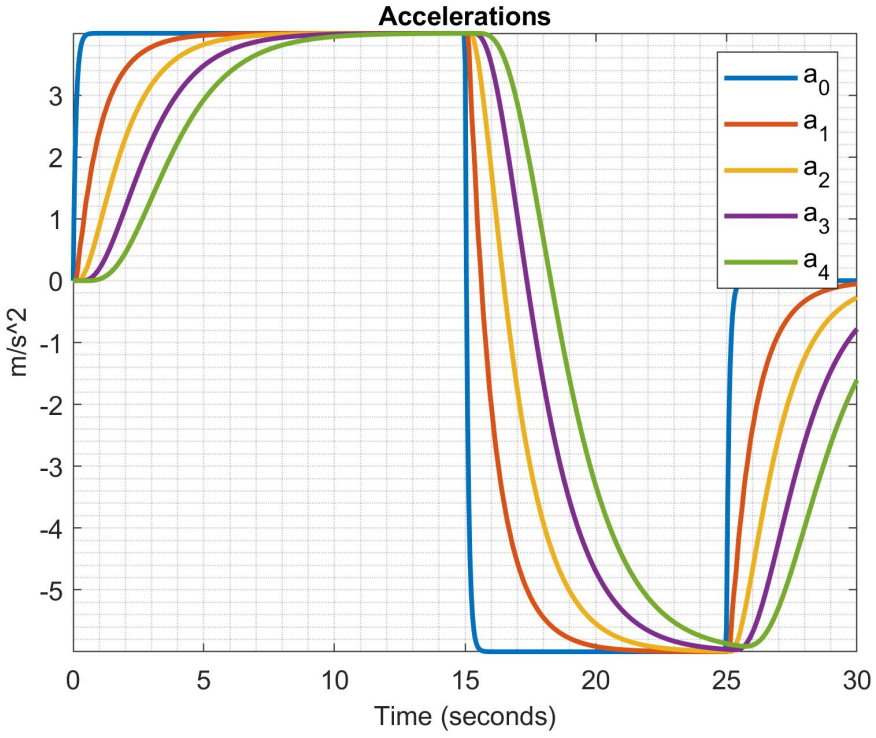


Figure 4.44: Accelerations for the controller in case 6 for 50ms actuator delay

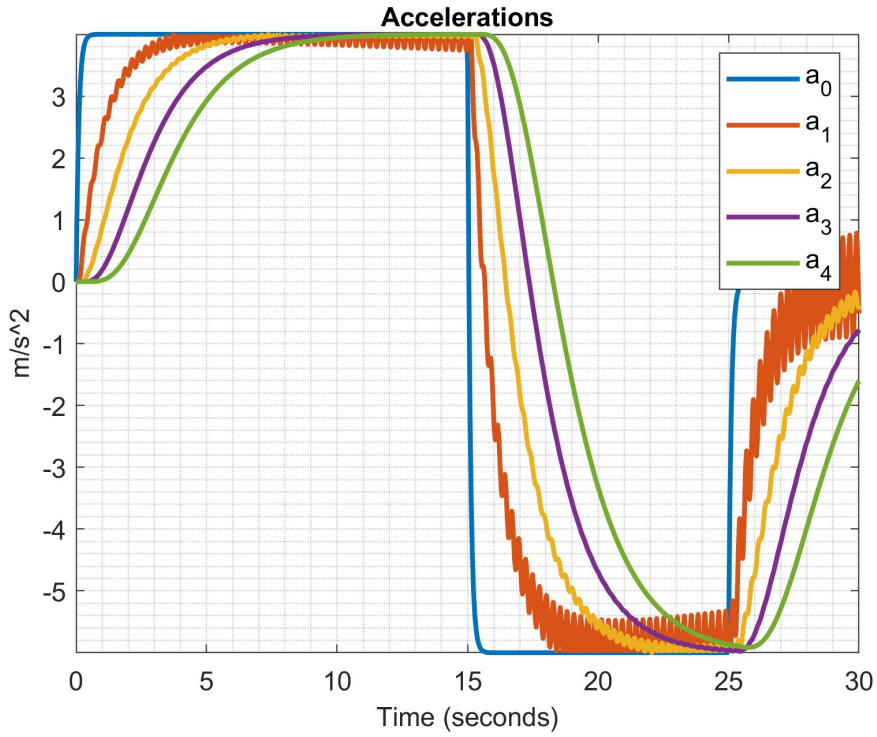


Figure 4.45: Accelerations for the controller in case 6 for 65ms actuator delay

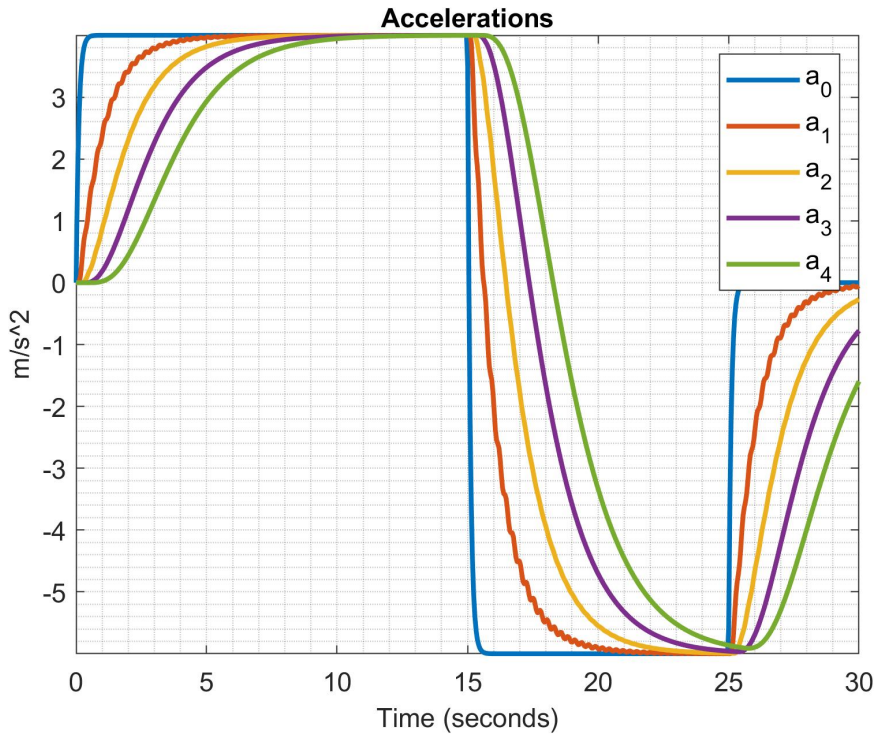


Figure 4.46: Accelerations for the controller in case 3 for 65ms actuator delay

In the following simulations, we are going to elaborate on the trade-off made by allowing greater headway time constants. Basically, allowing a greater headway time constant is not sought since it is one of the fundamental objectives of the whole CACC scheme, that is, by decreasing the intervehicle gap higher efficiency in traffic is wanted to be obtained. Yet, to be able to tolerate inherent delays, which cannot be decreased below certain values, one has to consider resolving this issue by increasing $h_i$ whenever a controller becomes incapable of handling them.

| $i$ | $h_i$ | $\theta_i$ | $\phi_i$ | $\tau_i$ |
|---|---|---|---|---|
| 0 | 0.5 | 0.02 | 0.065 | 0.30 |
| 1 | 0.5 | 0.02 | 0.065 | 0.31 |
| 2 | 0.5 | 0.02 | 0.065 | 0.32 |
| 3 | 0.5 | 0.02 | 0.065 | 0.33 |
| 4 | 0.5 | 0.02 | 0.065 | 0.34 |

Table 4.7: Fixed parameter set for examining the effect of headway time

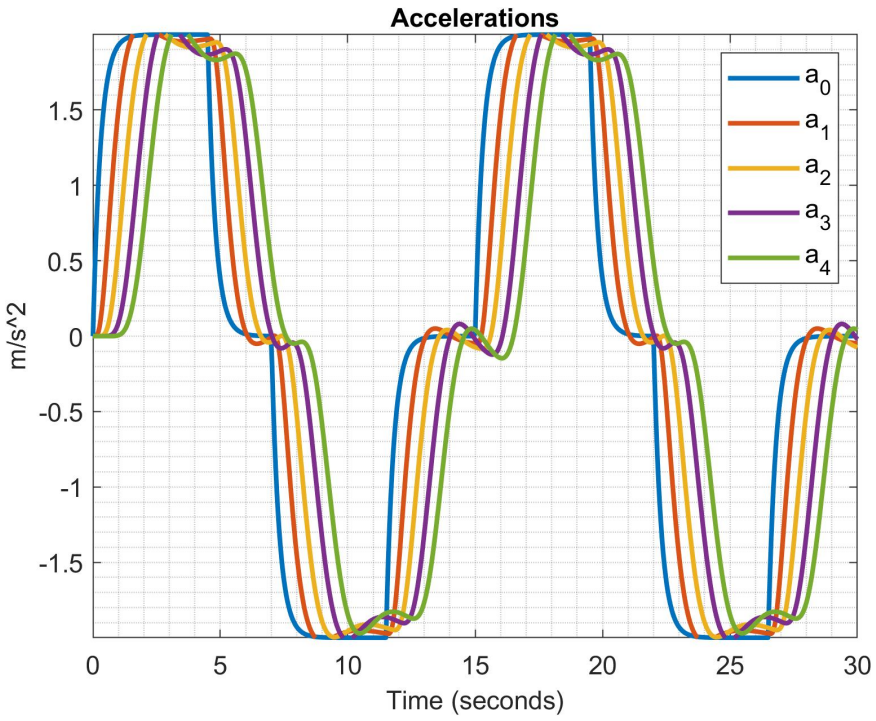


Figure 4.47: Accelerations for 0.5 second headway time

Simulation results for the values given in Table 4.7 with the input signal in Figure 4.5

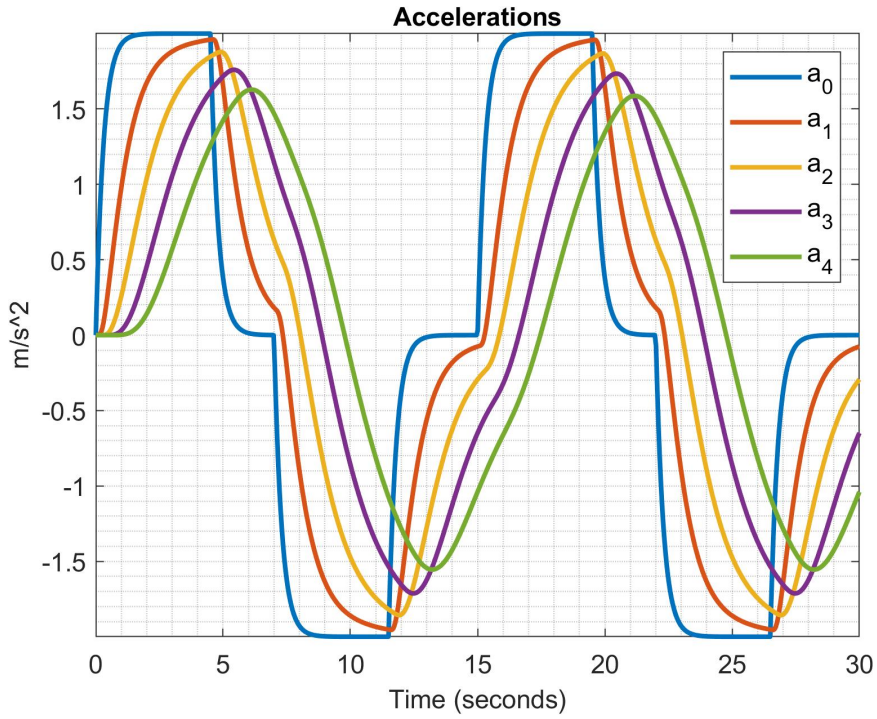


Figure 4.48: Accelerations for 1 second headway time

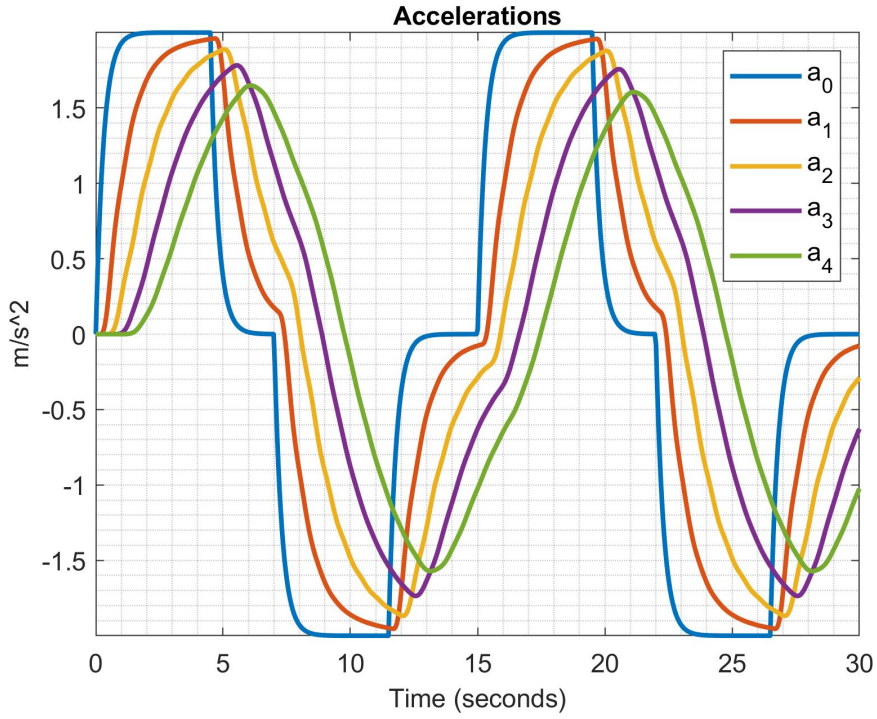


Figure 4.49: Accelerations for 1 second headway time 150ms actuator delay

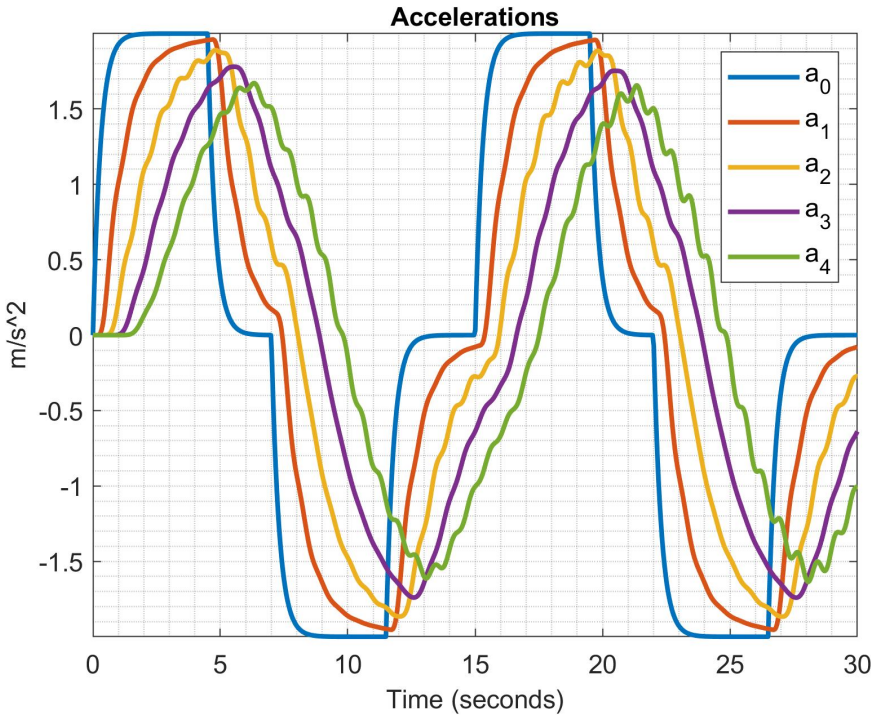


Figure 4.50: Accelerations for 1 second headway time 170ms actuator delay

are shown in Figure 4.47. It is seen that the system cannot attenuate the accelerations along the string. Now consider the exact same scenario, but with the headway time doubled. Then the response of the system becomes as seen in Figure 4.48. It is evident that the string has become stabilized compared to the response with $0.5s$ headway time. This is the effect of increase in headway time.

To see how much more of an actuator delay can be tolerated with the doubled headway time constant, 1 second, we simulated up to delays which drive the system string unstable. In Figures 4.49 and 4.50, it is observed that up to 150 milliseconds actuator delays there were no unstable behaviour in the acceleration signals, but beyond 170 milliseconds delay the string is unable to follow each other stably.

# CHAPTER 5

# CONCLUSION

With the advancement in many research areas, autonomous vehicles are, step by step, becoming a reality in daily life. CACC as being a subarea of research in this cutting edge technology, promises what is expected from future traffic dynamics. To clarify, sustainability has become the most trending concept in the last few decades due to the consequences of new millennium's people's lifestyle. In everything used or consumed by mass populations, it is the uttermost property to be asked since the future of humanity is endangered by what they cost physically. Hence, one of the very fundamental needs of almost entire population on the surface of earth, the traffic and transportation, has to be seized in an efficient and environment-friendly way. If the whole traffic phenomena was to be analyzed to see what portion of its pollution comes from longitudinal vehicle dynamics it would be evident that it constitutes the major component. Therefore, bringing the future vehicles' longitudinal motion controllers under the spotlight and developing the best possible solution becomes worthy of putting academical efforts on.

In this thesis work, we introduced a new methodology into CACC design literature by taking on an unexampled path for synthesizing controllers with one of the strongest types of strict $L_\infty$ string stability. As the initial step of our work, we formulated a sufficient condition for strict $L_\infty$ string stability based on a fundamental result by Laguerre. Then, we showed that these conditions can be used to define constraints for an optimization problem that determines the CACC controller parameters for achieving strict $L_\infty$ string stability. After validating the correctness of our method by simulation results, we further showed that the inevitable delays in actuators and communication can be tolerated up to a certain point, and the system robustness can be enhanced

by trading off with increments in headway time. The formulated optimization problem proved itself to be a novel way of designing controllers, in that, just by giving the standard known parameters as input to it, string stable CACC controllers can be obtained as its output.

Future works to be built upon this study will explicitly consider the delays in the controller design method for example by defining the delays with Padé approximations. Hereby, it has to be stressed that this is a challenging task according to our experience. Moreover, the proposition for alternating series sums may be generalized to apply the same theoretical work to the most generic cases in CACC where poles will not need to be forced to have zero complex parts during optimization process. Lastly, objective function to be defined during optimization process is a wide open subarea to be studied for any betterment.

# REFERENCES


[1] J. Ploeg, N. van de Wouw, and H. Nijmeijer, "Lp string stability of cascaded systems: Application to vehicle platooning," *IEEE Transactions on Control Systems Technology*, vol. 22, no. 2, pp. 786–793, 2014.

[2] J. Eyre, D. Yanakiev, and I. Kanellakopoulos, "A simplified framework for string stability analysis of automated vehicles," *Vehicle System Dynamics*, vol. 30, pp. 375–405, 1998.

[3] K. C. Dey, L. Yan, X. Wang, Y. Wang, H. Shen, M. Chowdhury, L. Yu, C. Qiu, and V. Soundararaj, "A review of communication, driver characteristics, and controls aspects of cooperative adaptive cruise control (cacc)," *IEEE Transactions on Intelligent Transportation Systems*, vol. 17, no. 2, pp. 491–509, 2016.

[4] S. Darbha, S. Konduri, and P. R. Pagilla, "Benefits of v2v communication for autonomous and connected vehicles," *IEEE Transactions on Intelligent Transportation Systems*, vol. 20, no. 5, pp. 1954–1963, 2019.

[5] H. Xing, J. Ploeg, and H. Nijmeijer, "Compensation of communication delays in a cooperative acc system," *IEEE Transactions on Vehicular Technology*, vol. 69, no. 2, pp. 1177–1189, 2020.

[6] Z. Wang, Y. Bian, S. E. Shladover, G. Wu, S. E. Li, and M. J. Barth, "A survey on cooperative longitudinal motion control of multiple connected and automated vehicles," *IEEE Intelligent Transportation Systems Magazine*, vol. 12, no. 1, pp. 4–24, 2020.

[7] J. Ploeg, B. T. M. Scheepers, E. van Nunen, N. van de Wouw, and H. Nijmeijer, "Design and experimental evaluation of cooperative adaptive cruise control," in *2011 14th International IEEE Conference on Intelligent Transportation Systems (ITSC)*, pp. 260–265, 2011.

[8] I. Bayezit, T. Veldhuizen, B. Fidan, J. Huissoon, and H. Lupker, "Design of

string stable adaptive cruise controllers for highway and urban missions," in *Communication, Control, and Computing (Allerton), 2012 50th Annual Allerton Conference on*, pp. 106–113, Oct 2012.

[9] J.-N. Meier, A. Kailas, O. Abuchaar, M. Abubakr, R. Adla, M. Ali, G. Bitar, R. Deering, U. Ibrahim, P. Kelkar, V. Vijaya Kumar, E. Moradi-Pari, J. Parikh, S. Rajab, M. Sakakida, and M. Yamamoto, "On augmenting adaptive cruise control systems with vehicular communication for smoother automated following," *Transportation Research Record: Journal of the Transportation Research Board*, vol. 2672, p. 036119811879637, 09 2018.

[10] D. Swaroop, *String stability of interconnected systems: An application to platooning in automated highway systems*. PhD thesis, University of California, Berkeley, 1994.

[11] S. Darbha, S. Konduri, and P. R. Pagilla, "Vehicle platooning with constant spacing strategies and multiple vehicle look ahead information," *IET Intelligent Transport Systems*, vol. 14, no. 6, pp. 589–600, 2020.

[12] G. J. L. Naus, R. P. A. Vugts, J. Ploeg, M. J. G. van de Molengraft, and M. Steinbuch, "String-stable cacc design and experimental validation: A frequency-domain approach," *IEEE Transactions on Vehicular Technology*, vol. 59, no. 9, pp. 4268–4279, 2010.

[13] J. Ploeg, D. P. Shukla, N. van de Wouw, and H. Nijmeijer, "Controller synthesis for string stability of vehicle platoons," *IEEE Transactions on Intelligent Transportation Systems*, vol. 15, no. 2, pp. 854–865, 2014.

[14] A. M. H. Al-Jhayyish and K. W. Schmidt, "Feedforward strategies for cooperative adaptive cruise control in heterogeneous vehicle strings," *IEEE Transactions on Intelligent Transportation Systems*, vol. 19, no. 1, pp. 113–122, 2018.

[15] Z. Wang, G. Wu, and M. J. Barth, "A review on cooperative adaptive cruise control (cacc) systems: Architectures, controls, and applications," in *2018 21st International Conference on Intelligent Transportation Systems (ITSC)*, pp. 2884–2891, 2018.

[16] Y. Zhu, D. Zhao, and Z. Zhong, "Adaptive optimal control of heterogeneous cacc system with uncertain dynamics," *IEEE Transactions on Control Systems Technology*, vol. 27, no. 4, pp. 1772–1779, 2019.

[17] Y. Zhou, M. Wang, and S. Ahn, "Distributed model predictive control approach for cooperative car-following with guaranteed local and string stability," *Transportation Research Part B: Methodological*, vol. 128, pp. 69–86, 2019.

[18] R. Rajamani, *Vehicle Dynamics and Control*. Springer US, 2012.

[19] C. Wang and H. Nijmeijer, "String stable heterogeneous vehicle platoon using cooperative adaptive cruise control," in *2015 IEEE 18th International Conference on Intelligent Transportation Systems*, pp. 1977–1982, 2015.

[20] J. Ploeg, E. Semsar-Kazerooni, G. Lijster, N. van de Wouw, and H. Nijmeijer, "Graceful degradation of cooperative adaptive cruise control," *IEEE Transactions on Intelligent Transportation Systems*, vol. 16, no. 1, pp. 488–497, 2015.

[21] S. Stankovic, M. Stanojevic, and D. Siljak, "Decentralized overlapping control of a platoon of vehicles," *IEEE Transactions on Control Systems Technology*, vol. 8, no. 5, pp. 816–832, 2000.

[22] S. Sheikholeslam and C. Desoer, "Longitudinal control of a platoon of vehicles with no communication of lead vehicle information: a system level study," *IEEE Transactions on Vehicular Technology*, vol. 42, no. 4, pp. 546–554, 1993.

[23] S. Feng, Y. Zhang, S. E. Li, Z. Cao, H. X. Liu, and L. Li, "String stability for vehicular platoon control: Definitions and analysis methods," *Annual Reviews in Control*, vol. 47, pp. 81–97, 2019.

[24] E. Laguerre, "On the theory of numeric equations," *Journal de Mathematiques pures et appliquees*, 1883.

[25] E. Schechter, "The cubic formula."

[26] "Ars magna (the great art)," in *Tales of Mathematicians and Physicists*, pp. 1–26, Springer New York.

[27] W. R. Inc., "Mathematica, Version 12.3.1." Champaign, IL, 2021.